9-26-2015

Deeply Dredged Submarine HIMU Glasses from the Tuvalu Islands, Polynesia: Implications for Volatile Budgets of Recycled Oceanic Crust

M. G. Jackson

K. T. Koga

A. Price

J. G. Konter

A. A.P. Koppers

See next page for additional authors

Follow this and additional works at: https://digitalcommons.uri.edu/gsofacpubs

Deeply Dredged Submarine HIMU Glasses from the Tuvalu Islands, Polynesia: Implications for Volatile Budgets of Recycled Oceanic Crust

Publisher Statement

Authors

M. G. Jackson, K. T. Koga, A. Price, J. G. Konter, A. A.P. Koppers, V. A. Finlayson, K. Konrad, E. H. Hauri, A. Kylander-Clark, Katherine A. Kelley, and M. A. Kendrick

Terms of Use

RESEARCH ARTICLE

Key Points:
- We report geochemical data on the first deeply dredged submarine glasses with a HIMU signature
- The HIMU glasses have low H2O/Ce
- The low H2O/Ce is interpreted to relate to mantle recycling of pyroxenite

Correspondence to:
M. G. Jackson,
jackson@geol.ucsb.edu

Deeply dredged submarine HIMU glasses from the Tuvalu Islands, Polynesia: Implications for volatile budgets of recycled oceanic crust

M. G. Jackson[1], K. T. Koga[2], A. Price[1], J. G. Konter[3], A. A. P. Koppers[4], V. A. Finlayson[3], K. Konrad[4], E. H. Hauri[5], A. Kylander-Clark[1], K. A. Kelley[6], and M. A. Kendrick[7]

[1]Department of Earth Science, University of California, Santa Barbara, California, USA, [2]Laboratoire Magmas Et Volcans, Universite Blaise Pascal, CNRS UMR 6524, Clermont-Ferrand, France, [3]Department of Geology and Geophysics, School of Earth and Ocean Sciences and Technology, University of Hawaii, Manoa, Honolulu, Hawaii, USA, [4]College of Earth, Ocean and Atmospheric Sciences, Oregon State University, Corvallis, Oregon, USA, [5]Department of Terrestrial Magnetism, Carnegie Institution of Washington, Washington, District of Columbia, USA, [6]Graduate School of Oceanography, University of Rhode Island, Narragansett, Rhode Island, USA, [7]Research School of Earth Sciences, Australian National University, Canberra, ACT, Australia

Abstract Ocean island basalts (OIB) with extremely radiogenic Pb-isotopic signatures are melts of a mantle component called HIMU (high μ, high $^{238}U/^{204}Pb$). Until now, deeply dredged submarine HIMU glasses have not been available, which has inhibited complete geochemical (in particular, volatile element) characterization of the HIMU mantle. We report major, trace and volatile element abundances in a suite of deeply dredged glasses from the Tuvalu Islands. Three Tuvalu glasses with the most extreme HIMU signatures have F/Nd ratios (35.6 ± 3.6) that are higher than the ratio ($\sim$21) for global OIB and MORB, consistent with elevated F/Nd ratios in end-member HIMU Mangaia melt inclusions. The Tuvalu glasses with the most extreme HIMU composition have Cl/K (0.11–0.12), Br/Cl (0.0024), and I/Cl (5–6×10^{-5}) ratios that preclude significant assimilation of seawater-derived Cl. The new HIMU glasses that are least degassed for H_2O have low H_2O/Ce ratios (75–84), similar to ratios identified in end-member OIB glasses with EM1 and EM2 signatures, but significantly lower than H_2O/Ce ratios (119–245) previously measured in melt inclusions from Mangaia. CO_2-H_2O equilibrium solubility models suggest that these HIMU glasses (recovered in two different dredges at 2500–3600 m water depth) have eruption pressures of 295–400 bars. We argue that degassing is unlikely to significantly reduce the primary melt H_2O. Thus, the lower H_2O/Ce in the HIMU Tuvalu glasses is a mantle signature. We explore oceanic crust recycling as the origin of the low H_2O/Ce ($\sim$50–80) in the EM1, EM2, and HIMU mantle domains.

1. Introduction

The Earth's mantle, as sampled by lavas erupted at mid-ocean ridges and hotspots, is isotopically heterogeneous. Much of this heterogeneity is thought to result from geochemical depletion by melt extraction (at mid-ocean ridges, subduction zones, and hotspots) and by injection of heterogeneous materials (such as altered oceanic crust and sediment) into the mantle at subduction zones [e.g., *Gast et al.*, 1964; *White and Hofmann*, 1982; *Hofmann and White*, 1982; *Zindler et al.*, 1982; *Zindler and Hart*, 1986; *Hart*, 1988; *Hofmann*, 1997; *White*, 2010]. Several isotopic end-members—including DMM (depleted MORB mantle), EM1 (enriched mantle I), EM2 (enriched mantle II), and HIMU (high $\mu = {}^{238}U/^{204}Pb$)—have been identified in basalts erupted at mid-ocean ridges (MORB) and ocean island basalts (OIB) erupted at hotspots [*Zindler and Hart*, 1986; *Hofmann*, 1997; *Stracke et al.*, 2005; *White*, 2010]. These isotopic end-members have been linked to different lithospheric materials (oceanic crust, oceanic mantle lithosphere, and sediments) subducted into the mantle in the geologic past, which are returned ("recycled") to the shallow mantle and melted beneath oceanic hotspot volcanoes and erupted as OIBs [*Cohen and O'Nions*, 1982; *Hofmann and White*, 1982; *White and Hofmann*, 1982]. For example, subducted upper continental crust is suggested to give rise to the EM2 mantle end-member [*White and Hofmann*, 1982; *Jackson et al.*, 2007; *Workman et al.*, 2008], but the origin of EM1 is not as well understood [*Weaver*, 1991; *Eiler et al.*, 1995; *Gasperini et al.*, 2000; *Eisele et al.*, 2002; *Honda and Woodhead*, 2005; *Geldmacher et al.*, 2008; *Salters and Sachi-Kocher*, 2010; *Collerson et al.*, 2010; *Hart*, 2011; *Konter and Becker*, 2012; *Garapic et al.*, 2015]. The HIMU mantle end-member is characterized by the

most radiogenic Pb-isotopic compositions in the oceanic mantle, and is thought to originate from recycling of ancient subducted oceanic crust [e.g., *Chase*, 1981; *Hofmann and White*, 1982; *Zindler et al.*, 1982; *Nakamura and Tatsumoto*, 1988; *Dupuy et al.*, 1989; *Graham et al.*, 1992; *Hauri and Hart*, 1993; *Hémond et al.*, 1994; *Roy-Barman and Allègre*, 1995; *Woodhead*, 1996; *Hanyu and Kaneoka*, 1997; *Kogiso et al.*, 1997; *Salters and White*, 1998; *Schiano et al.*, 2001; *Lassiter et al.*, 2003; *Stracke et al.*, 2003; *Stroncik and Haase*, 2004; *Kelley et al.*, 2005; *Nishio et al.*, 2005; *Chan et al.*, 2009; *Parai et al.*, 2009; *Day et al.*, 2009, 2010; *John et al.*, 2010; *Hanyu et al.*, 2011, 2014; *Kawabata et al.*, 2011; *Salters et al.*, 2011; *Krienitz et al.*, 2012; *Cabral et al.*, 2013, 2014]. Alternative mechanisms for generating the HIMU mantle have been proposed, including metasomatism, melting of lower mantle phases, and carbonate recycling [*Niu and O'Hara*, 2003; *Pilet et al.*, 2008; *Collerson et al.*, 2010; *Castillo*, 2015]. Complete geochemical characterization of the mantle end-member compositions is required to constrain their origins and to understand the geodynamic processes that preserve these heterogeneities over geologic time.

Fresh, deeply erupted (>1000 mbsl, meters below sea level) basaltic glasses, which are formed when erupting submarine lavas quench to glass upon contact with seawater, are critical for constraining the compositions and origins of mantle domains sourcing OIB volcanism. A primary reason for this is because glasses provide a means to visually evaluate freshness: fresh submarine volcanic glasses can preserve original magmatic compositions that can be used to "see through" posteruptive weathering processes that operate on basalts, as the groundmass of basalts can undergo alteration that is difficult to evaluate by visual inspection. Additionally, submarine volcanic glasses are critical for determining liquid compositions of magmas, which are difficult to infer from nonglass whole-rock lavas that often host phenocrysts. Finally, glasses are crucial for evaluating the volatile inventories of magmas as well as the stable isotopic compositions of volatile elements. Subaerially erupted lavas are typically highly degassed of their complement of volatile species, making it difficult to infer the undegassed primary magmatic volatile contents and their primary magmatic isotopic compositions. Deeply erupted basalt glasses better preserve their complement of volatile elements, and such glasses are therefore critical for investigating the volatile budgets of magmas.

Constraining the volatile budgets of the mantle end-members is critical because volatiles affect the depth and extent of mantle melting, the composition of subsequent melts, and how they evolved during crystallization processes [e.g., *Kushiro et al.*, 1968; *Gaetani and Grove*, 1998; *Asimow and Langmuir*, 2003; *Asimow et al.*, 2004; *Hirschmann*, 2006; *Dasgupta and Hirschmann*, 2006; *Portnyagin et al.*, 2007]. While fresh, deeply dredged glasses are available for end-member lavas representing the EM1 (from Pitcairn) and EM2 (from Societies and Samoa) mantle domains, which have been characterized for their respective volatile budgets [*Workman et al.*, 2006; *Kendrick et al.*, 2014, 2015], the community still lacks deeply dredged glasses with end-member HIMU compositions. This owes, in large part, to a lack of deep sea dredging campaigns targeting the flanks of oceanic hotspot volcanoes known to have HIMU signatures. While volcanic glasses with HIMU compositions have been recovered during shallow submersible dives on the islands of Rurutu and Tubuai, low CO_2 concentrations (due to relatively shallow eruption and recovery) in these HIMU glasses provide evidence that the lavas also may have experienced some loss of H_2O by degassing [*Nichols et al.*, 2014a], making it difficult to infer the H_2O abundance in the undegassed HIMU primary melts.

The lack of fresh, deeply dredged HIMU glass has been an impediment to developing a more complete understanding of the HIMU mantle. The recovery of the glasses reported here is important because volatile budgets of the HIMU mantle are critical for the generation of melts of this end-member [*Jackson and Dasgupta*, 2008; *Dasgupta et al.*, 2007, 2009; *Gerbode and Dasgupta*, 2010; *Mallik and Dasgupta*, 2012, 2014], and the volatile budgets of HIMU lavas may provide clues to how volatiles are cycled through the mantle, from subduction zones to hotspots [*Cabral et al.*, 2014]. During residence on the seafloor, the uppermost portion of oceanic crust undergoes low-temperature alteration and incorporation of volatiles (including several weight percent H_2O and CO_2) [*Staudigel et al.*, 1996; *Alt and Teagle*, 1999; *Bach et al.*, 2001; *Wallmann*, 2001; *Dixon et al.*, 2002; *Gillis and Coogan*, 2011]. If the HIMU mantle forms by subduction and long-term storage of altered oceanic crust that is cycled through the mantle and melted beneath hotspots, then melts of HIMU mantle domains provide important constraints on volatile cycling in the mantle. Such constraints include insights into volatile loss from the slab during subduction and how volatiles are retained in the subducted slab during long-term storage in the mantle. Obtaining better constraints on the volatile budgets of
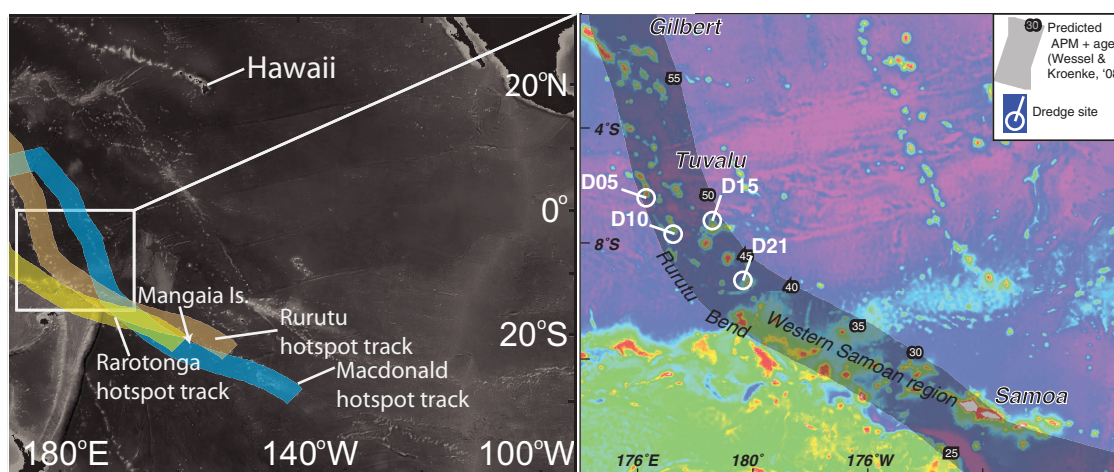
Figure 1. A bathymetric map of southwest Pacific, showing reconstructed path of the Rurutu hotspot and the locations of the new dredge samples in the Tuvalu Island chain. The Rurutu hotspot track reconstruction is anchored to Arago seamount [*Bonneville et al.*, 2002, 2006] and uses the *Wessel and Kroenke* [2008] plate motion model. The Rurutu hotspot reconstruction follows earlier plate reconstructions for the Rurutu hotspot shown in *Konter et al.* [2008] and *Jackson et al.* [2010]. The four dredge locations in the Tuvalu Islands that yielded glass are indicated. The reconstructed hotspot tracks for two other hotspots in the Cook-Austral volcanic lineament, the Macdonald and Rarotonga hotspots, are also shown (and are after *Chauvel et al.* [1997] and *Konter et al.* [2008]); Mangaia Island formed as part of the Macdonald hotspot [*Chauvel et al.*, 1997]. In the inset, the reconstructed path of the Rurutu hotspot is also shown; numbers on the hotspot track reconstruction represent modeled ages in Ma. This reconstructed path coincides with the trace of the Tuvalu Island chain.

the HIMU mantle domain becomes a possibility with the recovery of a suite of fresh, deeply dredged HIMU glasses that we analyze in this study.

During the 2013 cruise of the R/V *Roger Revelle* (Expedition RR1310), the deep submarine flanks of volcanoes in the Tuvalu Islands and seamounts (Figure 1) were targeted for a systematic dredging campaign to prospect for geochemical signatures of Late Cretaceous to Early Paleogene HIMU hotspot volcanism. The Tuvalus are proposed to define an older (~50–70 Ma) segment of the Rurutu hotspot track [*Konter et al.*, 2008], which is anchored to its eastern (young) end by Arago seamount (which has lavas as young as 230 ka) [*Bonneville et al.*, 2002, 2006]. Arago seamount is located in the Austral volcanic lineament, and the youngest subaerial lavas along the Rurutu hotspot outcrop near Arago seamount on Rurutu Island [*Chauvel et al.*, 1997]. West of the Cook-Austral Islands, the Rurutu hotspot track should exhibit a hotspot "bend" at ~50 Ma, similar to the Hawaii-Emperor bend (HEB) (Figure 1) [*Konter et al.*, 2008], where the Tuvalus mark the segment of the Rurutu hotspot track erupted just prior to (and north of) its HEB-like bend. To the north and west of the Tuvalus, the Rurutu hotspot extends back in time through the Gilbert Ridge atolls (erupted between 64 and 70 Ma) [*Koppers et al.*, 2007] and the Western Pacific Seamount Province (WPSP) that may extend Rurutu HIMU-type hotspot volcanism back >100 Ma [*Staudigel et al.*, 1991; *Koppers et al.*, 2003; *Konter et al.*, 2008].

The systematic RR1310 dredging campaign conducted as part of this study sought to obtain additional basaltic material from the portion of the Rurutu hotspot occupied by the Tuvalu Islands and seamounts. A major goal of the expedition was to determine whether the HIMU signature has been continuous over time, particularly over the portion of the hotspot erupted just prior to the Rurutu hotspot's HEB-like bend [*Finlayson et al.*, 2014] (Figure 1). Four out of 26 successful dredges from the Tuvalus yielded fresh, glassy basaltic material. Here we report new Pb-isotopic data indicating that glasses from two of these dredges have clear HIMU signatures that exceed the magnitude of HIMU signatures previously reported in lavas from the Rurutu hotspot (Figure 1). In addition, we report a full suite of geochemical data obtained on these HIMU glasses, including their volatile, major and trace element compositions, thus providing new insights into the geochemistry of the HIMU mantle, which we explore below.

2. Sample Description and Methods Introduction

The glasses reported in this study were recovered by deep-sea dredging on Expedition RR1310 of the R/V *Roger Revelle*. Sample locations and dredge depths are reported in supporting information Table S1 and shown in Figure 1. All dredges were made at depths between ~2500 and ~3900 mbsl. Dredge tracks were

generally quite long (up to 1 km in length) to improve the success of recovering volcanic rock during each dredge. Therefore, the dredges span a vertical swath of approximately 1000 m along the submarine flanks of the Tuvalu Islands and seamounts (see supporting information Table S1).

The glasses were recovered from four volcanoes in the Tuvalu chain and range in age from 64–47 Ma (with the exception of dredge 21, which has an age of 8.8 Ma) [*Konrad et al.*, 2014]. Dredges targeted fault scarps that expose the interiors of the volcanic edifices, which may explain the preservation of fresh volcanic glass after such long-time periods on the seafloor. However, the glassy portions from each sample were extremely limited, ranging from a few milligrams to tens of milligrams of material. The largest glass samples were recovered in samples from dredges 15 and 21, which preserve only small pockets of fresh glassy material embedded in the rims of pillow basalts, and much of the volcanic glass has undergone palagonatization. Samples recovered in dredges 5 and 10 preserve rare submillimeter-sized shards of fresh glass hosted in a matrix of highly altered hyaloclastite; these glass shards preserve material that has neither experienced palagonitization nor devitrification. Following isolation from the respective hand samples, select glass samples from all four dredges were placed in an indium mount [see *Cabral et al.*, 2014 for methods] for subsequent analysis.

Owing to the extremely small quantities of glassy material available for characterization, microbeam techniques were employed for generating the geochemical data whenever possible. However, we did succeed in separating small quantities of glass from two samples in dredge 10, which was used for combined Cl, Br, and I measurement by the noble gas method [*Kendrick*, 2012; *Kendrick et al.*, 2013]. The compositions of reference glasses measured during the course of this study are provided in supporting information Table S2, and the combined Cl, Br, and I data obtained by the noble gas method are shown in supporting information Table S3. All analytical techniques that were used in this study are described in detail in the supporting information.

3. Results

The most important finding reported in this paper is the discovery of HIMU isotopic signatures in deeply erupted volcanic glasses from dredges 5 and 10 in the Tuvalu Islands (Figure 1). Other geochemical data presented on the Tuvalu volcanic glasses, including major, trace and volatile element concentrations, are presented in light of this unique isotopic signature. Additional glasses were recovered from two other dredges in the cruise (dredges 15 and 21) that do not possess the extreme HIMU geochemical signatures observed in dredges 5 and 10. While the glasses from these two dredges are not the focus of this paper, the data for these glasses are presented for completeness.

3.1. Pb-Isotopic Characteristics of the Tuvalu Lavas

The new Pb-isotopic data on the Tuvalus submarine glasses are reported in supporting information Table S1. The data are presented in a plot of $^{208}Pb/^{206}Pb$ versus $^{207}Pb/^{206}Pb$ (Figure 2). This isotopic projection resolves the mantle isotopic end-members (EM1, EM2, HIMU, and MORB) and has long been used for Pb-isotopic data sets obtained by in situ techniques on oceanic lavas when ^{204}Pb data are not available [e.g., *Saal et al.*, 1998; *Yurimoto et al.*, 2004; *Cabral et al.*, 2014].

The new Pb-isotopic data set on the Tuvalu lavas reveals that glasses from two different islands (dredge 5 and dredge 10) host lavas with extreme HIMU signatures, one (dredge 15) has moderate HIMU signatures and another one (dredge 21) does not have a HIMU signature. However, dredge 10 has heterogeneous Pb-isotopic compositions: while three glasses from dredge 10 have extreme HIMU signatures, two glasses from this dredge have only mild HIMU signatures, very similar to those found in dredge 15 (described below). These two glasses from dredge 10 are referred to as "mildly-HIMU" glasses hereafter. The other three glass samples from dredge 10 have the most extreme HIMU signatures observed in this study. In fact, the HIMU signatures in dredge 10 lavas are more extreme than any previously observed in lavas related to the portion of the Rurutu-hotspot that erupted along the Cook-Austral volcanic lineament (Figure 2), which include lavas from Atiu Island, Mauke Island, the younger series of lavas from Rurutu Island, Arago seamount, and a seamount sampled near Rimatara (dredge 2 of the ZEPOLYF2 cruise) [*Bonneville et al.*, 2006]. While the dredge 10 Tuvalu HIMU glasses do have fairly extreme HIMU signatures, they do not have Pb-isotopic compositions as extreme as those identified in whole rock lavas from Mangaia Island in the Cook Islands, which represent the most extreme HIMU signatures identified in global OIBs. However, the HIMU
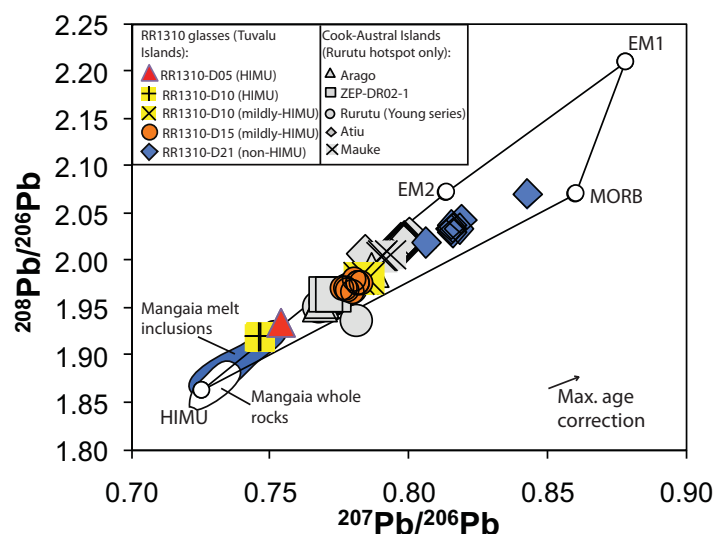
Figure 2. $^{208}Pb/^{206}Pb$ versus $^{207}Pb/^{206}Pb$ isotopic compositions of lavas associated with the Rurutu hotspot. The Pb-isotopic data measured on glasses in the four dredges from the Tuvalu Islands examined in this study are shown in color (error bars are smaller than the data points). Pb-isotopic compositions on lavas collected from volcanoes associated with the Rurutu hotspot in the Cook-Austral chain are shown as gray symbols: Atiu, Rurutu (young series), Mauke, Arago seamount, and dredge 2 of the ZEPOLYF2 (i.e., ZEP-DR02-1) cruise from *Bonneville et al.* [2006]. (Note that the older series of lavas at Aitutake Island are considered to be part of the Rurutu hotspot [*Chauvel et al.*, 1997], but Pb-isotopic data from this lava series are not available). Data are compiled from Georoc (http://georoc.mpch-mainz.gwdg.de/georoc/), and exclude data from *Palacz and Saunders* [1986] owing to potential sample contamination [*McDonough and Chauvel*, 1991]. The new glasses reported here encompass a wider range of Pb-isotopic compositions (including a more extreme HIMU composition) than identified in Rurutu-hotspot lavas sampled from the Cook-Austral volcanic lineament. Mangaia is not part of the Rurutu hotspot, but it represents the most extreme HIMU compositions found in the ocean basins. Therefore, the field for the freshest Mangaia lavas analyzed with highest-precision techniques (i.e., multicollector ICP-MS) is also shown (field after that defined in *Cabral et al.* [2014]). The field of olivine-hosted Mangaia melt inclusions is from *Cabral et al.* [2014]. The arrow indicates the magnitude and direction of the maximum age correction (applicable to dredge 15 lavas with the highest U/Pb and Th/Pb ratios), which slightly reduces the apparent magnitude of the HIMU signature; age corrections are smaller for all other glasses.

lavas from dredge 10 do have Pb-isotopic compositions that overlap with the olivine-hosted HIMU melt inclusions separated from Mangaia lavas [*Cabral et al.*, 2014] (Figure 2). We note that the comparison with Mangaia is only to provide geochemical context, however, as Mangaia is a product of a different hotspot (the Macdonald hotspot) in the Cook-Austral volcanic chain (Figure 1).

Dredge 5 glasses have slightly weaker HIMU signatures than those observed in dredge 10, but the HIMU signatures are more extreme than observed in Rurutu hotspot-related lavas erupted in the Cook-Austral volcanic chain (Figure 2).

Glasses from dredge 15 form a tight cluster in Pb-isotopic space and do not exhibit the extreme HIMU signatures observed in dredges 5 and 10 (Figure 2). Instead, these lavas plot midway between the HIMU and EM2 end-members in Pb-isotopic space and have a moderate radiogenic Pb-isotope signature similar to the subset of glasses from dredge 10 that have mildly HIMU signatures.

Of the glasses reported in this study, the glasses from dredge 21 plot furthest from the HIMU mantle end-member in Pb-isotopic space. In Figure 2, dredge 21 glasses plot in the region between the EM2 and MORB end-members. Notably, dredge 21 glasses exhibit no overlap with Rurutu hotspot-related volcanoes from the Cook-Austral volcanic lineament. Instead, dredge 21 lavas form an array that begins near compositions identified in Atiu lavas (a Rurutu hotspot-related island in the Cook-Austral chain) and extends toward a component with higher $^{208}Pb/^{206}Pb$ and $^{207}Pb/^{206}Pb$. The observation that dredge 21 lavas exhibit no isotopic overlap with lavas from the Cook-Austral chain may relate to the younger ~9 Ma ages [*Konrad et al.*, 2014] reported in lavas from this seamount, which is ~40 Ma younger than lavas dredged from nearby volcanoes in the Tuvalus. This suggests that, unlike the other samples from the Tuvalu Islands examined here, dredge 21 lavas are unrelated to the Rurutu hotspot, and sample a mantle source unlike that seen in the main shield-building stages of volcanism in the Cook-Austral chain.

Radiogenic ingrowth since eruption of the glasses does not significantly affect the primary observations made in this study. While none of the glass samples have been dated, dates obtained on other lavas from dredge 21 (~9 Ma) and dredge 15 (~50 Ma) can be used for age correction calculation. Lavas from dredges 5 and 10 are unsuitable for age dating. However, they are predicted to have ages of 56 and 51 Ma, respectively, if they fall on the Rurutu hotspot age progression. Employing these ages, the maximum age corrections to the $^{207}Pb/^{206}Pb$ and $^{208}Pb/^{206}Pb$ ratios measured in the glasses reported here are 1.4% and 0.6% of the Pb-isotopic ratios, respectively, and are shown graphically in Figure 2. Employing the maximum age

correction, the glasses with the most extreme HIMU signatures (from dredge 10) in this study remain more extreme than other Rurutu hotspot-related lavas (Figure 2).

3.2. Major Element Characteristics of Tuvalu Lavas

Major element compositions are reported in supporting information Table S1. In a plot of total alkalis versus SiO_2, the Tuvalu submarine glasses are generally alkalic [*Macdonald and Katsura*, 1964], similar to lavas from the Cook-Austral volcanic lineament associated with the Rurutu hotspot track (Figure 3). However, the two mildly HIMU glasses from dredge 10 are tholeiitic, in contrast to the remaining three glasses from dredge 10, which are alkalic and exhibit the most extreme HIMU Pb-isotopic compositions in this study. All dredge 15 glasses and most of the dredge 21 glasses are alkali basalts (however, a single dredge 21 glass, D21-03, is a tephrite basanite). The dredge 5 glasses are tephrite basanites, as is a single HIMU glass from dredge 10. Two of the remaining HIMU glasses from dredge 10 are trachybasalts. Finally, the two moderately HIMU glasses from dredge 10 are tholeiitic basalts.

Compared to dredge 10 glasses, glasses from dredges 5, 15, and 21 exhibit more homogeneous intradredge major element compositions. However, one glass from dredge 21 (sample D21-03) is compositionally (and isotopically) distinct, with a total alkali content approximately twice as high as other glasses from this dredge (other incompatible trace elements, including fluid immobile trace elements, are also significantly higher in this sample; see section 3.3).

Major element variation plots show that the Tuvalu glasses have relatively low MgO (<8.2 wt.%) (Figure 3). The glasses generally cluster in a narrow range of SiO_2 concentrations (45.1–47.6 wt.%), with the exception of the two tholeiitic glass samples from dredge 10, which have higher SiO_2 (∼52 wt.%). Plots of FeO and TiO_2 versus MgO reveal that the glasses have FeO and TiO_2 concentrations that plot at the lower end of, or below, concentrations observed in whole rock lavas from the Cook-Austral volcanic lineament that are related to the Rurutu hotspot. The new glasses exhibit lower CaO/Al_2O_3 with diminishing MgO. Low CaO/Al_2O_3 in lavas with low MgO is a common feature among lavas from the Cook-Austral volcanic lineament (Figure 3), and reflects clinopyroxene (cpx) fractionation at low MgO [e.g., *Jackson and Dasgupta*, 2008]. K_2O (and to a lesser degree Na_2O) exhibits increasing concentrations as MgO decreases, indicating that these alkali elements behave incompatibly during crystal fractionation processes operating during magma evolution.

The most extreme HIMU glasses, from dredges 5 and 10, also have the lowest MgO observed in this study. Extreme EM1 and EM2 glasses from Pitcairn and Societies seamounts, respectively, were also shown to exhibit low MgO abundances [*Devey et al.*, 2003].

3.3. Trace Element Characteristics of Tuvalu Glasses

Trace element concentrations are reported in supporting information Table S1. Like K_2O, the concentrations of Ce and Nb increase with decreasing MgO in the Tuvalu glasses (Figure 4). The behavior of other highly incompatible lithophile elements analyzed in this study (e.g., Ba, Rb, Th, etc., not shown) mirror Ce and Nb. In contrast, weakly compatible trace elements such as Sc, show decreasing concentrations with decreasing MgO, consistent with partitioning of Sc into cpx as these magmas evolve and the cpx is lost by fractional crystallization (which is consistent with diminished CaO/Al_2O_3 with decreasing MgO; Figure 3). Ni also shows decreasing concentrations with decreasing MgO, which can result from olivine, cpx, and Ni-rich sulfide fractionation. Cu shows scattered, but generally decreasing concentrations with decreasing MgO in the glass; Cu is highly chalcophile, and this pattern is consistent with S partitioning from glass into sulfide, and is consistent with magma evolution during sulfide-saturated conditions.

Primitive mantle (PM) [*McDonough and Sun*, 1995] normalized incompatible trace element patterns in the Tuvalu glasses exhibit significant variability (Figure 5). The glasses with the most extreme HIMU Pb-isotopic signatures, all from dredges 5 and 10 (which also have the lowest MgO reported in this study), are the most enriched in highly incompatible elements in the glass suite reported here. Both glasses from dredge 5 have similar trace element patterns. The three extreme HIMU glasses from dredge 10 are similar to each other, but are less enriched in highly incompatible elements than dredge 5 glasses. However, the two mildly HIMU tholeiitic glasses from dredge 10 are less enriched in incompatible trace elements than the three extreme HIMU glasses from this dredge. The dredge 15 glasses, which have Pb-isotopic signatures like the mildly HIMU dredge 10 glasses, exhibit remarkably homogeneous trace element patterns; these glasses have MgO
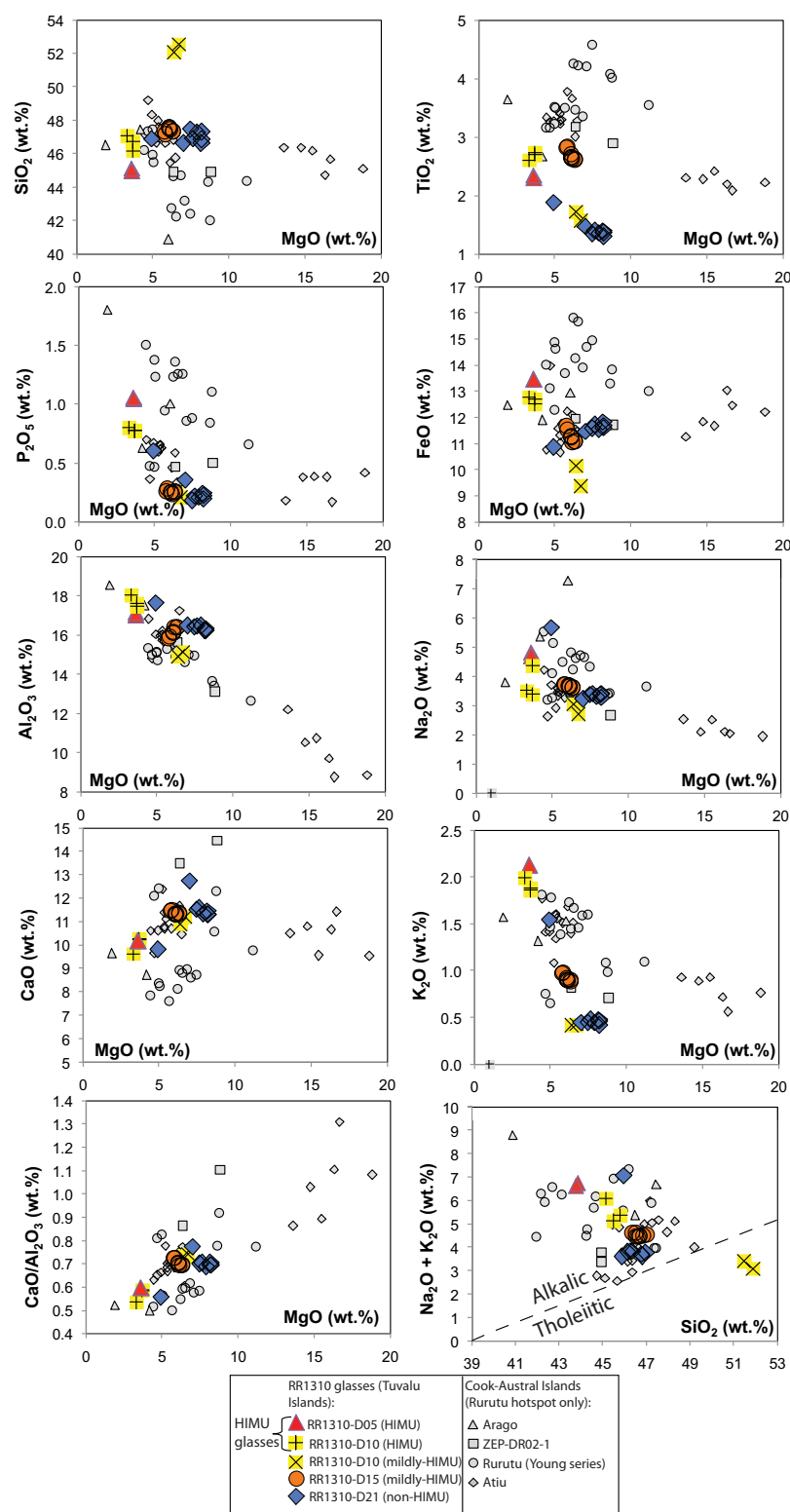
Figure 3. Major element variation diagrams. The major element compositions of glasses from the Tuvalu Islands are plotted together with whole rock major element data on lavas collected from islands and seamounts associated with the Rurutu hotspot in the Cook-Austral chain: Atiu, Rurutu (young series), Arago seamount, and dredge 2 of the ZEPOLYF2 cruise from *Bonneville et al.* [2006]; major element data from Aitutake (old series) and Mauke are not available. Whole rock major element data are compiled from Georoc (http://georoc.mpch-mainz.gwdg.de/georoc/). All major element data are reported on a dry basis normalized to 100% totals.
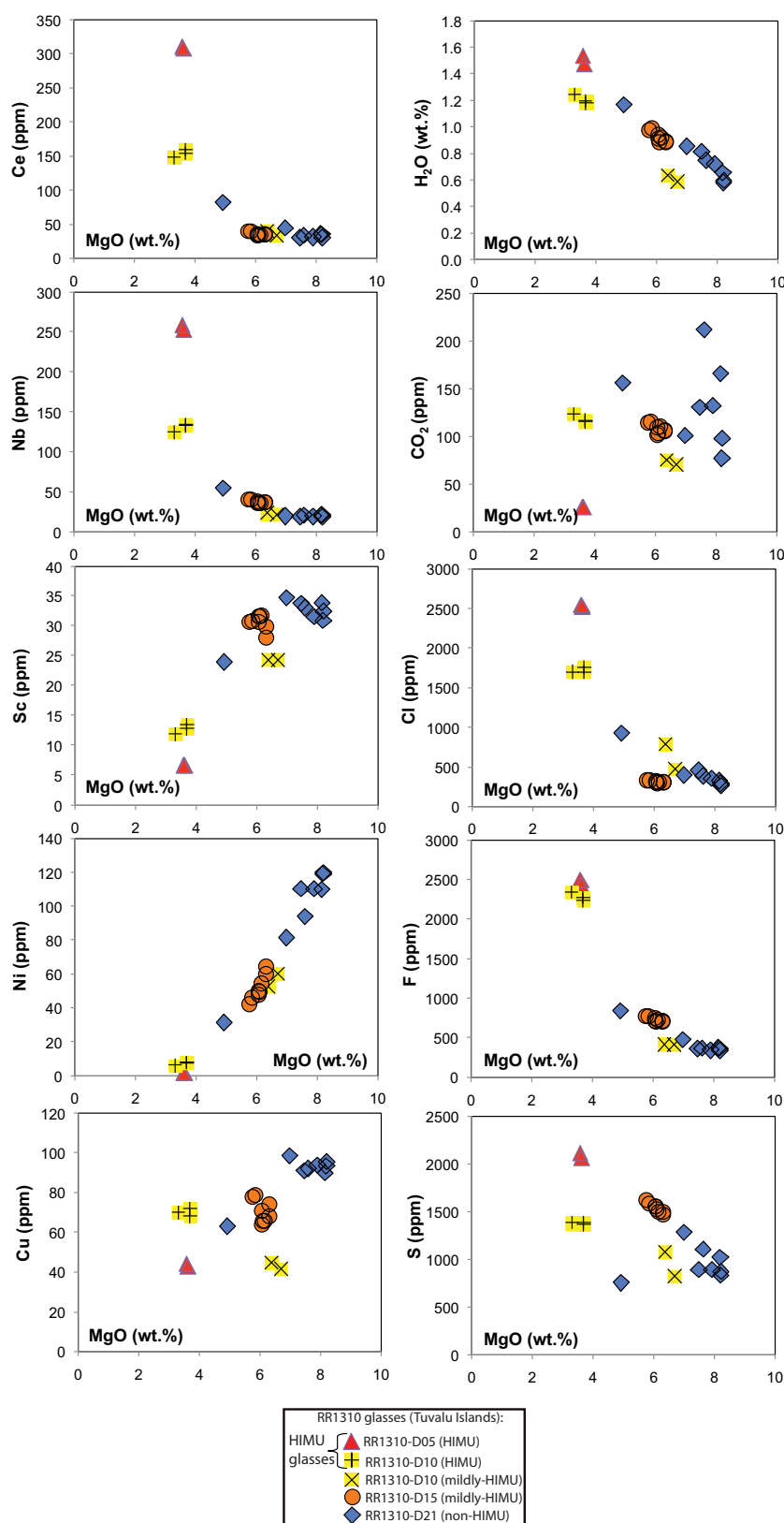
Figure 4. Trace and volatile element concentrations versus MgO. The data are from the new Tuvalu glasses and presented in supporting information Table S1.
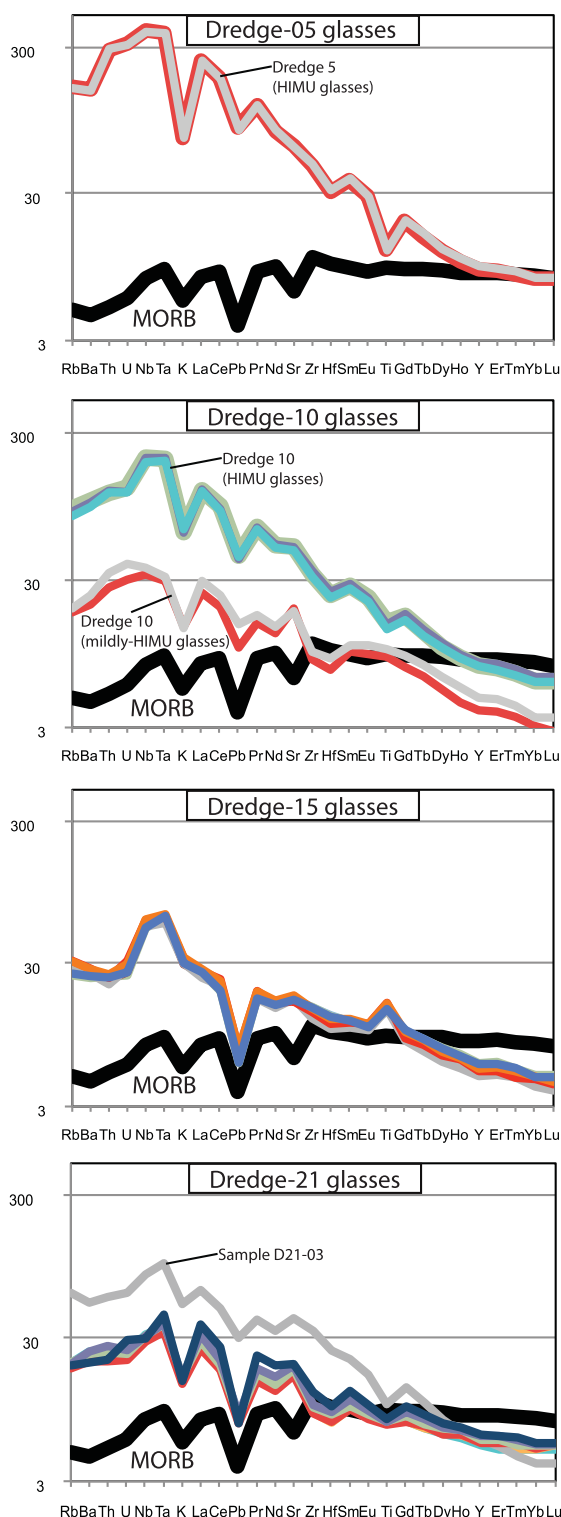
Figure 5. Primitive mantle normalized trace element patterns for the Tuvalu glasses reported here. Each plot presents data obtained on glasses from a single dredge, and data from glasses analyzed from four dredges (5, 10, 15, and 21) are shown in the figures. In several cases, the trace element composition of the glasses are quite similar and the trace element patterns are indistinguishable. The average MORB composition from *Gale et al.* [2013] is shown for reference. The primitive mantle composition from *McDonough and Sun* [1995] is used for normalization.

that is in the middle of the range identified in the Tuvalu glasses in this study and exhibit PM-normalized trace element patterns that are less enriched in the highly incompatible elements than the HIMU glasses from dredges 5 and 10. Finally, with the exception of a single glass sample, the glasses from dredge 21 have relatively homogeneous trace element patterns, exhibit the highest MgO in this study, and have a level of incompatible trace element enrichment that is comparable to dredge 15 lavas. However, a single exceptional glass sample from dredge 21 (sample D21-03) has higher incompatible trace element concentrations and lower MgO than the other glasses from the same dredge; the incompatible element enrichment in this glass is consistent with its elevated total alkali content relative to the other glasses from dredge 21.

3.4. H_2O and CO_2 in Tuvalu Glasses

H_2O and CO_2 concentrations are reported in supporting information Table S1. H_2O concentrations range from 0.58 to 1.54 wt.% in the Tuvalu glasses, and are ≥ 1.18 wt.% in the glasses with the strongest HIMU signatures from dredges 5 and 10 (Figure 6). CO_2 concentrations range from 26 to 212 ppm in the Tuvalu glass suite. In a plot of H_2O versus MgO (Figure 4), H_2O concentrations increase with decreasing MgO, typical of an incompatible element during increasing degrees of magmatic differentiation. Unlike H_2O, CO_2 exhibits scattered concentrations with decreasing magmatic MgO, likely owing to degassing and loss of CO_2 from the melt during magmatic evolution.

H_2O and CO_2 concentrations measured in the glasses can be used to estimate the eruption depths of the Tuvalu glasses (Figure 6). The SolEx [*Witham et al.*, 2012] CO_2-H_2O equilibrium solubility model is used to estimate the depth of H_2O-CO_2 vapor saturation, and to infer the water depths of eruption of the glasses in this study. Using a composition specific to the HIMU glasses from dredge 5, the CO_2-H_2O solubility model is consistent with eruption depths of 240–260 bars. The three alkalic glasses
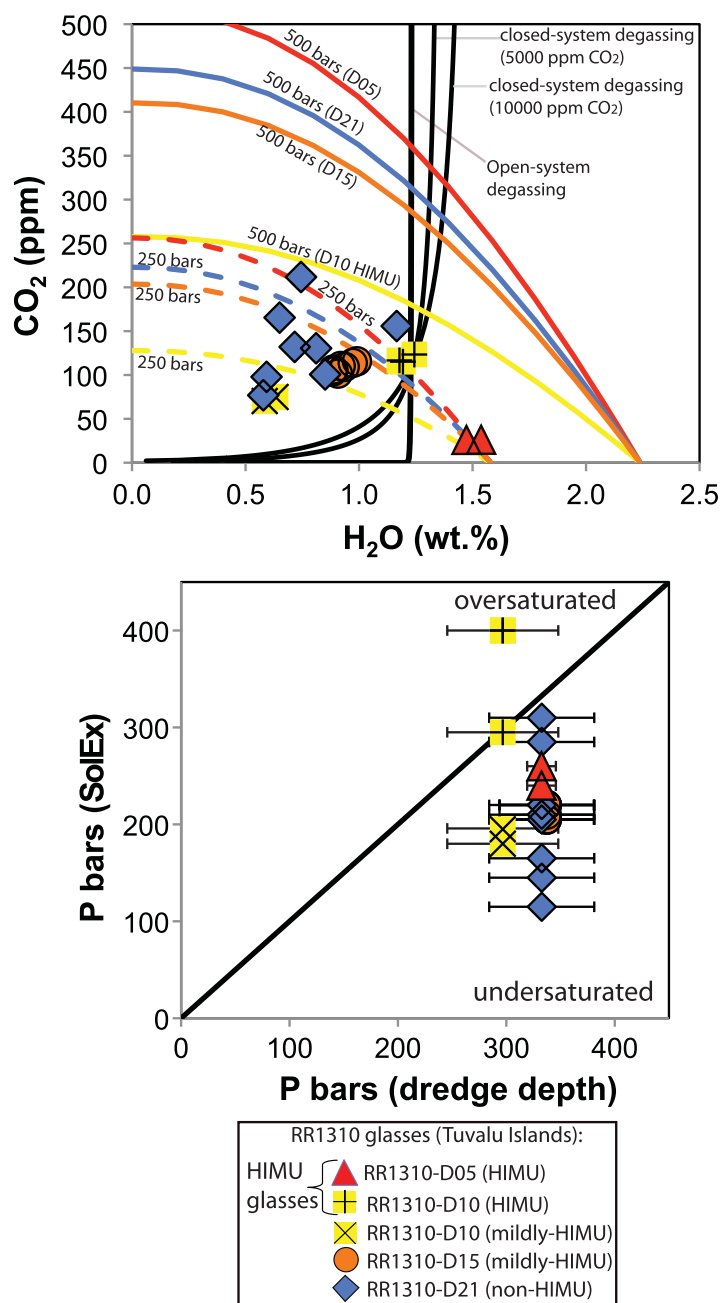
Figure 6. Relationships between H_2O and CO_2 in Tuvalu glasses. (top) Isobars are calculated at two different pressure intervals (250 (dashed color lines) and 500 (solid color lines) bars) using the SolEx software assuming a temperature of 1160°C [*Witham et al.*, 2012]. Four isobars at each pressure interval are calculated using the average major element compositions measured in each of the dredge groups: dredge 10 HIMU glasses (yellow lines), dredge 5 glasses (red lines), dredge 15 glasses (orange lines), and dredge 21 glasses (blue lines, excluding the highly alkalic sample from dredge 21). Isobars for the dredge 10 mildly HIMU glass are not shown, but they are similar to the dredge 10 HIMU glasses. Model degassing trends are shown for extreme HIMU glass D10–33, as described in the text: open and closed-system degassing trends are shown for initial CO_2 concentrations of 5000 and 10,000 ppm. (bottom) H_2O-CO_2 equilibrium saturation pressures for the glass samples are compared to dredge depths. While the maximum and minimum dredge depths (represented by the error bars) for each dredge are known, the exact dredge depths for each sample reported here are not precisely known. In most cases, dredge tracks in the Tuvalus were long (material was collected over 1 vertical km along the side of an island; supporting information Table S1), and the error bars represent the range in possible dredge depths.

with extreme HIMU compositions from dredge 10 preserve H_2O and CO_2 concentrations consistent with an eruption depth range of 295–400 bars; the H_2O-CO_2 equilibrium solubility pressures of the high SiO_2, tholeiitic compositions in the mildly HIMU glasses from dredge 10 are calculated to be 180–195 bars. The glasses from dredge 15 record H_2O-CO_2 equilibrium solubility pressures of 205–220 bars, whereas glasses from dredge 21 span a wide range of eruption pressures, from 115 bars to 310 bars.

3.5. Sulfur and Halogens in Tuvalu Glasses

F, Cl, and S concentrations are reported in supporting information Table S1. F (339–2502 ppm), Cl (265–2551 ppm), and S (751–2117 ppm) concentrations exhibit significant variability in the suite of glasses examined here. F and Cl exhibit increasing concentrations with decreasing MgO, which is consistent with highly incompatible behavior during magmatic differentiation (Figure 4). However, S exhibits more scattered behavior, and does not exhibit a clear relationship with decreasing MgO (Figure 4). This may result, in part, from degassing. However, S will behave as a compatible element during magmatic differentiation if sulfide is saturated in the melt. The scattered behavior of S might also result from sulfide fractionation, a hypothesis that is consistent with reduced Cu concentrations with decreasing MgO in the Tuvalu glasses. This contrasts with increasing Nb concentrations with decreasing MgO (Figure 4), behavior that is expected by an incompatible element during magmatic differentiation. In fact, ratios of Cu to other incompatible elements (e.g., Cu/Nb, not shown) show decreasing values with decreasing MgO. These trends are best explained by sulfide fractionation
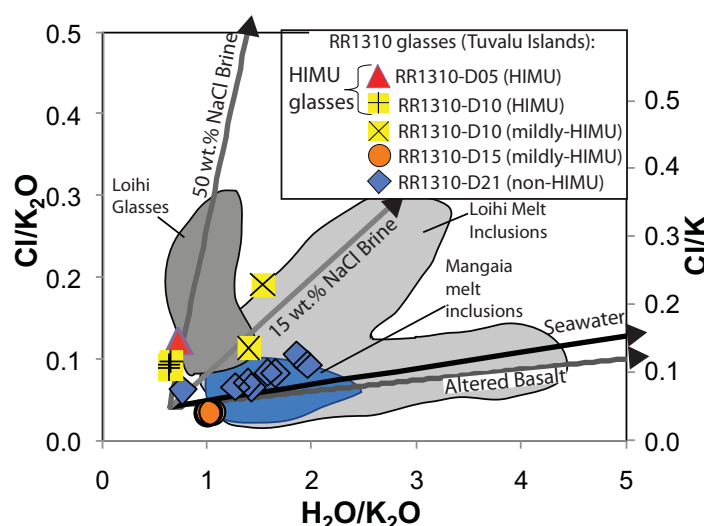
Figure 7. Cl/K_2O (and Cl/K) versus H_2O/K_2O for the new Tuvalu glasses. Data for the new Tuvalu glasses are shown with model mixing curves that illustrate the effects of assimilation of altered oceanic crust, seawater, and brines (15 wt.% and 50 wt.% NaCl brines). The Cl/K_2O and H_2O/K_2O of pristine mantle melts (unaffected by assimilation of seawater-derived Cl or H_2O) is poorly defined, but is situated toward the bottom left of the diagram. Slopes are shown emanating from a point with H_2O/K_2O of 0.65 and Cl/K_2O of 0.4, to illustrate the relative affects of assimilating brines of variable salinity (15 wt.% NaCl and 50 wt.% NaCl), seawater and altered oceanic crust. Similar models have been described previously, and the mixing model shown here uses the same assimilant end-members provided in Kent et al. [1999a,b]. The field for Mangaia melt inclusions [Cabral et al., 2014] excludes samples that have lost H_2O by diffusion through the host olivine (i.e., all inclusions from sample MGA-B-47); fields for Loihi glasses and melt inclusions, which provide examples of melts that have experienced assimilation, based on data from Kent et al. [1999a,b], are shown for reference.

during magmatic differentiation. Owing to the possibility of sulfide saturation in the HIMU glasses, which would cause the concentration of S in the glasses to be buffered by the presence of sulfide, S is not further discussed in this paper.

Previous work has suggested a significant portion of the Cl present in basalt glass can be introduced by assimilation of seawater components, and this can overprint the mantle-derived Cl [Michael and Cornell, 1998; Kent et al., 1999a,b,; Kendrick et al., 2013, 2015]. The presence of seawater-derived Cl introduced by assimilation of altered oceanic crust, seawater, or seawater-derived brines can be explored using a plot of Cl/K_2O (and Cl/K) versus H_2O/K_2O (see Figure 7 and section 4.1.2). In the current study, the mildly HIMU lavas from dredge 10 have elevated Cl/K of up to ~0.23 that lies between nominal mixing trajectories described by assimilation of 15% and 50% brines (Figure 7). In comparison, glasses from dredges 15 and 21 have Cl/K of 0.04–0.13, glasses with a HIMU signature from dredge 5 have Cl/K of 0.15, and the dredge 10 glasses with the strongest HIMU signatures in this study have Cl/K of 0.11–0.12. The key observation is that the glasses with the most extreme HIMU signatures have Cl/K ratios that are within or close to the range typical of mantle melts that have not assimilated seawater-derived Cl [Michael and Cornell, 1998; Kendrick et al., 2012].

Furthermore, samples D10-36 and D10-48 have Br/Cl (2.4×10^{-3}) and I/Cl ($5–6 \times 10^{-5}$) ratios that are within the range considered typical of the mantle, which is (2.8 ± 0.6) $\times 10^{-3}$ and (60 ± 30) $\times 10^{-6}$, respectively [Kendrick et al., 2012] (supporting information Table S3). I and Br data are not available for the other glasses in this study.

F/Nd ratios of the glasses, which are considered to reflect mantle source compositions due to the similar incompatibility of these elements, vary from 18.5 to 38.7 (Figure 8). The F/Nd ratios do not correlate with Pb-isotopic compositions. It has previously been suggested that on a global basis, MORB, OIB and continental crust all have relatively constant F/Nd ratios of ~21 [Workman et al., 2006]. However, there is a relatively large uncertainty in the extent of variation around this canonical value, with MORB alone estimated to have an average F/Nd of 20 ± 12 (2σ) [Workman et al., 2006]. A high degree of variability in the F/Nd ratio is also found in the Tuvalu glasses. The three Tuvalu glass samples with the most extreme HIMU signatures in this study (from dredge 10) have F/Nd ratios of 36 ± 4 (2σ) that overlap with F/Nd ratios (30 ± 9) measured in end-member HIMU melt inclusions from Mangaia [Cabral et al., 2014]. However, high F/Nd ratios may not be a universal signature of HIMU lavas: Tuvalu glasses with slightly less extreme HIMU signatures, from Dredge 5, have F/Nd ratios (~24) that are closer to the canonical ratio suggested for global MORB and OIB. Also, lavas with relatively weak HIMU signatures—lavas from dredge 15—have high F/Nd ratios (37 ± 2). The mildly HIMU lavas from dredge 10, which have Pb-isotopic compositions similar to dredge 15 lavas, have low F/Nd of 24. Tuvalu glasses with the weakest HIMU signature in this study, from dredge 21, have the lowest F/Nd in this study (20 ± 1).
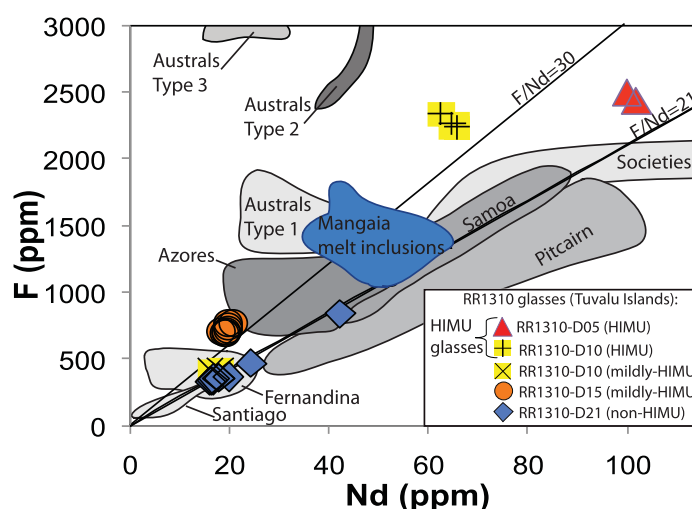
Figure 8. Relationships between F and Nd in Tuvalu glasses compared to global oceanic glasses and melt inclusions. Lines of constant F/Nd (F/Nd = 30 and F/Nd = 21) are shown for reference. Data fields for other oceanic lavas and melt inclusions from previous studies are shown for reference, and the data are from the following references: *Lassiter et al.* [2002]; *Workman et al.* [2006]; *Koleszar et al.* [2009]; *Kendrick et al.* [2014]; *Metrich et al.* [2014]. The Austral samples shown in the figure are melt inclusions that are divided among three categories (plotted as three distinct fields in the figure) according to *Lassiter et al.* [2002]: Type 1 inclusions are the most pristine (and have experienced the least assimilation); Type 2 inclusions are suggested to result from assimilation of Cl-rich brines; Type 3 inclusions are suggested to be secondary inclusions. The field for HIMU melt inclusions from Mangaia is defined by data published in *Cabral et al.* [2014]. Figure is modified after *Cabral et al.* [2014].

3.6. Relationships Between H_2O and Ce, H_2O/Ce, and Pb Isotopes

H_2O concentrations in the Tuvalu glasses form a rough positive trend when plotted against Ce concentrations (Figure 9). The two most extreme HIMU glass suites from the Tuvalus (from dredges 5 and 10) anchor the portion of the array with the highest H_2O and Ce concentrations (Figure 9). When compared to data obtained on extreme HIMU melt inclusions from Mangaia, the Tuvalu HIMU glasses (dredges 5 and 10) tend to have higher Ce at a given H_2O concentration (Figure 9). In Figure 9, the Tuvalu HIMU glasses plot either within the fields defined by EM1 and EM2 end-member glasses from

the Pitcairn, Societies, and Samoan hotspots, or along an extension of the trajectory defined by glasses from these hotspots. It is notable that, in the global OIB and MORB glass database, H_2O and Ce increase in tandem until H_2O concentrations reach ∼1.0–1.6 wt.% H_2O, at which point H_2O concentrations do not increase further but Ce concentrations continue to increase in the direction of the EM1 (Pitcairn) and EM2 (Society and Samoa) end-member lavas. As a result, lavas with end-member EM1 and EM2 compositions have low H_2O/Ce ratios (Figure 10). However, HIMU melts can have both high H_2O/Ce (as identified in HIMU melt inclusions from Mangaia) and low H_2O/Ce ratios (as identified in two different Tuvalu dredges with HIMU glass compositions).

In Figure 10, the H_2O/Ce ratios measured in the Tuvalu glasses are plotted against $^{208}Pb/^{206}Pb$ and $^{207}Pb/^{206}Pb$ ratios, which record mantle source compositions. The Tuvalu glasses with the strongest HIMU signatures have low $^{208}Pb/^{206}Pb$ and $^{207}Pb/^{206}Pb$ ratios and exhibit low H_2O/Ce ratios ranging from 49 (dredge 5) to 79 (dredge 10). This range of ratios is significantly lower than the range of H_2O/Ce ratios (119–245) observed in HIMU Mangaia melt inclusions that have not experienced diffusive water loss [*Cabral et al.*, 2014]. Looking ahead (see section 4.1.1), the dredge 5 HIMU glasses may be highly degassed for H_2O, and H_2O/Ce ratios of these glasses cannot reliably be used to infer the mantle source of HIMU. However, the low H_2O/Ce in the dredge 10 HIMU glasses is unlikely to be a feature attributable to degassing. While the H_2O/Ce ratios of the Mangaia HIMU inclusions [*Cabral et al.*, 2014] and HIMU Tuvalu glasses exhibit no overlap, it is notable that the most extreme HIMU Tuvalu glasses in this study, all from dredge 10, have $^{207}Pb/^{206}Pb$ (0.746–0.747) and $^{208}Pb/^{206}Pb$ (1.919–1.921) ratios that overlap with the range of $^{207}Pb/^{206}Pb$ (0.725–0.752) and $^{208}Pb/^{206}Pb$ (1.864–1.925) ratios measured in the Mangaia melt inclusions (Figure 2).

The Tuvalu glasses from dredges 15 and 21, and the mildly HIMU glasses from dredge 10, have either mild HIMU Pb-isotopic signatures or lack HIMU signatures altogether, and these glasses have higher H_2O/Ce ratios that range from 143 (dredge 21) to 282 (dredge 15).

4. Discussion

The submarine glasses from the Tuvalus represent the first suite of deeply dredged glasses (>2500 mbsl) with strong HIMU geochemical signatures, and this new suite of glasses provides an important
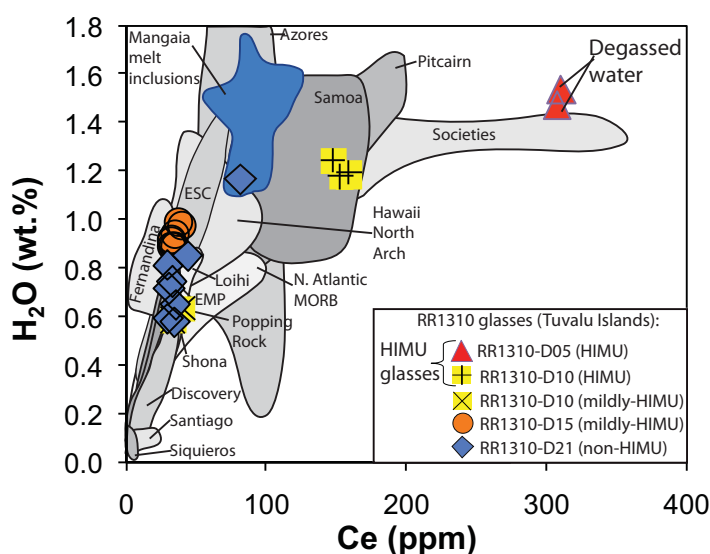
Figure 9. Relationships between H_2O and Ce in the Tuvalu glass suite compared to global OIB and MORB submarine glasses and melt inclusions. Data fields for other global OIB and MORB localities are from the following references: *Schilling et al.* [1985]; *Clague et al.* [1995]; *Douglass et al.* [1995]; *Dixon* [1997]; *Langmuir et al.* [1997]; *Pan and Batiza* [1998]; *Dixon and Clague* [2001]; *Dixon et al.*, [2002]; *Hauri* [2002]; *Kingsley* [2002]; *Saal et al.* [2002]; *Simons et al.* [2002]; *Yang et al.* [2003]; *le Roux et al.* [2002]; *Workman et al.* [2004], [2006]; *Cartigny et al.* [2008], and references therein; *Koleszar et al.* [2009]; *Kelley et al.* [2013]; *Kendrick et al.* [2014]; *Metrich et al.* [2014]. The figure is modified after *Cabral et al.* [2014], and methods for filtering the global database are provided in the same reference. The field for HIMU melt inclusions from Mangaia is defined by data published in *Cabral et al.* [2014], and excludes melt inclusions that have experienced diffusive H_2O-loss through the host olivine (i.e., all inclusions from sample MGA-B-47). EMP is Easter microplate and ESC is Easter seamount chain. Dredge 5 glasses from the Tuvalus may have degassed significant H_2O by closed-system degassing.

opportunity to constrain the volatile budgets of the HIMU mantle. Critically, these deeply dredged HIMU glasses provide a geochemical data set that can be compared with earlier work presenting volatile and trace element analyses on end-member HIMU melt inclusions from Mangaia (Cook Islands) [*Cabral et al.*, 2014]. A primary observation is that the H_2O/Ce ratios in the Tuvalu HIMU glasses range from 49 to 79 (from dredges 5 and 10, respectively), while the subset of olivine-hosted inclusions from Mangaia that have not experienced diffusive water loss (from the inclusion through the host olivine) have H_2O/Ce ratios that vary between 119 and 245 [*Cabral et al.*, 2014]. A key question is why the Mangaia melt inclusions exhibit higher H_2O/Ce ratios than the HIMU glasses, even though the two groups (Mangaia HIMU melt inclusions and HIMU Tuvalus glasses) exhibit overlapping Pb-isotopic compositions.

Constraining the H_2O/Ce ratio is critical, as this ratio in undegassed mantle melts (that have not experienced assimilation) is also considered to reflect the mantle source ratio, as H_2O and Ce are considered to be similarly incompatible during mantle melting [*Michael*, 1995; *Dixon et al.*, 2002]. We argue that the H_2O/Ce ratio measured in a subset of the Tuvalu glasses can help constrain the water content of the mantle. However, before we can consider the mechanism(s) responsible for the different H_2O/Ce between the Mangaia inclusions and the HIMU Tuvalu glasses, it is important to evaluate the various processes, including degassing and assimilation, that may have operated on the Tuvalu melts to modify the H_2O/Ce ratios.

4.1. Processes Operating on Tuvalu Melts
4.1.1. Degassing
CO_2 is highly insoluble in mantle melts and therefore CO_2 is undersaturated in basaltic glasses only in rare cases [i.e., *Saal et al.*, 2002]. However, in all other OIB and MORB lavas observed to date, CO_2 has been degassed and our suite of samples is no exception. Vapor saturation pressures estimated from H_2O-CO_2 solubility models indicate that the Tuvalu magmas were erupted at pressures ≥115 bars, consistent with their deep dredge depths (>2500 mbsl). In this context, it is important to evaluate the possible extent of H_2O loss via degassing. The degassing mechanism for CO_2 loss—open system versus closed system degassing—plays a central role in determining the extent to which H_2O is also degassed. The degassing models presented below for open system degassing are polybaric, and represent Raleigh degassing fractionation in which every infinitesimally small batch of gas leaves the system as soon as it forms. In the closed system degassing models, gas bubbles and magma ascend at the same rate and the compositions of the H_2O and CO_2 in the gas bubbles are constantly changing to be in equilibrium with the magma during ascent; in

Figure 10. H_2O/Ce versus $^{208}Pb/^{206}Pb$ and $^{207}Pb/^{206}Pb$ for Tuvalu glasses and global OIBs and MORBs. Data from other OIB and MORB sources are provided for comparison and consist of submarine glass samples and melt inclusions [*Staudigel et al.*, 1984; *Hanan and Schilling*, 1989; *Devey et al.*, 1990; *Dosso et al.*, 1991; *Fontignie and Schilling*, 1991; *Woodhead and Devey*, 1993; *Douglass et al.*, 1995; *Dixon*, 1997; *Kingsley and Schilling*, 1998; *Douglass et al.*, 1999; *Dosso et al.*, 1999; *Frey et al.*, 2000; *Dixon and Clague*, 2001; *Dixon et al.*, 2002; *Kingsley*, 2002; *Simons et al.*, 2002; *Yang et al.*, 2003; *Honda and Woodhead*, 2005; *Workman et al.*, 2006; *Cartigny et al.*, 2008, and references therein; *Hanyu et al.*, 2011; *Kelley et al.*, 2013]. In both plots, the field for HIMU melt inclusions from Mangaia is defined by data published in *Cabral et al.* [2014], and excludes melt inclusions that have experienced diffusive H_2O-loss through the host olivine (i.e., all inclusions from sample MGA-B-47). The HIMU mantle reservoir is sampled by both Mangaia melt inclusions and by dredge 10 HIMU glasses from the Tuvalus. Dredge 5 glasses from the Tuvalus may have degassed significant H_2O by closed-system degassing processes. The figure is modified after *Cabral et al.* [2014], and methods for filtering the global database are provided in the same reference.

closed system degassing, H_2O and CO_2 stay in the magma-bubble system until submarine eruption, then degassing occurs as a single monobaric event.

During open system degassing from great depth, the vapor phase is dominated by CO_2 and H_2O is not efficiently degassed, owing to the relatively high solubility of H_2O in basaltic melts at high pressure [*Dixon et al.*, 1995; *Dixon*, 1997; *Webster et al.*, 1999]. In contrast, during closed system degassing, the mass fraction of water in the vapor phase increases dramatically, particularly as the system reaches lower pressures, and H_2O can be efficiently degassed. However, near-vertical trends in CO_2 versus H_2O diagrams obtained by submarine glasses from various OIB localities globally (Samoa, Pitcairn, Societies, Hawaii, etc.) are interpreted to indicate that open-system degassing dominates over closed-system degassing until all but the lowest submarine eruption pressures (<100 bars) [e.g., *Dixon*, 1997; *Workman et al.*, 2006; *Kendrick et al.*, 2014]. In these cases, H_2O contents of the melts are interpreted to reflect the primary melt composition. Unfortunately, there is insufficient spread in CO_2 concentrations from the

Tuvalu samples to delineate the vertical trends observed at other OIB localities, so we cannot assume that degassing followed open-system behavior (Figure 6). In particular, the HIMU glasses from dredge 10 (n = 3 glasses) and dredge 5 (n = 2) do not provide a large number of samples to infer the degassing mechanism that operated on the glasses. Therefore, both open and closed-system degassing must be considered as possible degassing mechanisms operating on these melts. In addition, we must consider the fact that, compared to open-system degassing, the proportion of H_2O (relative to CO_2) in the vapor phase increases significantly at lower pressures during closed system degassing, and H_2O-loss from the melt can be significant. Additionally, the extent of H_2O loss to the vapor phase is a function of melt composition, in particular the initial CO_2 content, and higher initial (primary melt) CO_2 concentrations result in higher levels of closed-system H_2O degassing.

To constrain the role that closed-system degassing can play in modifying the H_2O content of the HIMU glasses from dredges 5 and 10, we model closed-system degassing with SolEx software [*Witham et al.*, 2012] assuming a magma temperature of 1160°C and the measured major element composition of the melts (using the "Π parameter" in SolEx) [*Dixon*, 1997]. In the model, two representative HIMU glass samples from each of the two dredges with HIMU glasses, D05–29 and D10–33, undergo closed-system degassing until the degassing model reached the H_2O and CO_2 concentrations measured in the two glasses, which occurs at pressures of 260 and 400 bars, respectively. The modeling effort explores the influence of different initial melt CO_2 concentrations on the degassing of H_2O, where higher initial CO_2 concentrations result in more extensive degassing of H_2O. Owing to the low measured CO_2 in the dredge 5 and 10 glasses, their initial CO_2 concentrations are not known. One approach to estimating the CO_2 concentration of a primary melt is to assume a constant CO_2/Nb ratio for undegassed primary melts [*Saal et al.*, 2002]. This approach is applied to the Tuvalu OIB melts to obtain a rough estimate of primary melt CO_2 concentrations. If a CO_2/Nb ratio of 300 is assumed for the primary melt [*Koleszar et al.*, 2009], and if a primary melt Nb concentration of 16–17 ppm is assumed (i.e., a range of values similar to Nb concentrations in Rurutu hotspot-related lavas that have 16% MgO), then the CO_2 concentration of the primary melt is 5000 ppm (0.5 wt.%).

Under the closed-system degassing conditions and 5000 ppm initial CO_2, the model results show that the D10–33 HIMU glass loses only ∼9% of its initial H_2O by the time it erupts on the seafloor at 400 bars water pressure. In contrast, D05–29 is calculated to erupt more shallowly (260 bars water pressure) and it degasses ∼54% of its initial H_2O. Clearly, the glasses in dredge 5 are highly degassed of their original H_2O complement if closed-system degassing has operated on these melts, and the H_2O contents of the dredge 5 glasses cannot reliably be used to infer the H_2O/Ce ratios of the primary melts. Therefore, H_2O and H_2O/Ce in dredge 5 glasses are not further considered in the discussion below. However, the degassing model shows that dredge 10 glasses have likely lost <10% of their initial H_2O, and the H_2O/Ce ratios measured in these glasses are thus similar to the primary melt ratios.

We acknowledge that the CO_2/Nb ratio of the HIMU mantle domain is not well constrained, and that CO_2/Nb ratios may be higher or lower than the value of 300 used above. Lower CO_2/Nb ratios for the HIMU source would result in low primary melt CO_2 and less degassing of H_2O. However, we consider it unlikely that the HIMU mantle domain has low CO_2. At least two lines of evidence suggest that the HIMU domain is CO_2 rich. First, HIMU peridotite mantle xenoliths with strong HIMU compositions from Tubuai Island exhibit evidence for metasomatism by a carbonatite fluid [*Hauri et al.*, 1993], highlighting the role of carbonatite in the genesis of this mantle end-member. Second, HIMU lavas have distinct major element compositions (including, e.g., low SiO_2 and high CaO/Al_2O_3) that are best explained by melting under CO_2-rich conditions [e.g., *Kushiro*, 1975; *Eggler*, 1978; *Dasgupta et al.*, 2004, 2007; *Jackson and Dasgupta*, 2008; *Gerbode and Dasgupta*, 2010; *Mallik and Dasgupta*, 2012, 2014].

If higher primary melt CO_2 concentrations of 10,000 ppm (1 wt.%) are assumed (which results in a CO_2/Nb ratio of 600) for the dredge 10 glasses with the most extreme HIMU compositions in this study, only ∼17% of the H_2O is calculated to have been lost by degassing, and the low H_2O/Ce in the dredge 10 glasses is still consistent with HIMU primary melts having low H_2O/Ce like EM1 and EM2 lavas from Pitcairn, Societies, and Samoa. Therefore, we conclude that degassing of H_2O is not the mechanism responsible for generating the low H_2O/Ce ratios in the dredge 10 HIMU Tuvalu lavas relative to the higher H_2O/Ce ratios in end-member HIMU melt inclusions from Mangaia [*Cabral et al.*, 2014]. Of course, the assumption of closed-system degassing offers a worst case scenario for H_2O loss by degassing from basaltic melts; for open-system degassing under the same conditions as assumed for the closed-system models above, only ∼1% H_2O loss is calculated for the dredge 10 HIMU lavas.

We acknowledge that complex, multistage degassing scenarios may lead to additional water depletion in HIMU melts. For example, *Blundy et al.* [2010] explore a range of degassing processes to evaluate related data sets for volatiles in melt inclusions from arc lavas, and argued that CO_2 addition to arc magmas at depth can enhance degassing. However, there are insufficient constraints in our data set (e.g., variation in CO_2 and H_2O in the two suites of HIMU glasses is quite limited) to explore these processes. Moreover, It is not clear that such a degassing mechanism is applicable to OIB melts examined here. For example, *Colin et al.* [2013] examined variability in He, Ar, and CO_2 concentrations in individual vesicles from several MORB glasses, and they found that the variability is consistent with Raleigh degassing.

Finally, the dredge depths can be compared with pressures calculated from a CO_2-H_2O equilibrium vapor saturation model, which may approximate eruption depths. Two HIMU lavas from dredge 10 have dredge depths that are lower than the eruption depths estimated from CO_2-H_2O equilibrium vapor saturation pressures. This apparent oversaturation in CO_2 may be due to an ascent rate that was too high to efficiently degas CO_2 [e.g., *Chavrit et al.*, 2012]. However, the dredge depths of the other glasses exceed the pressure calculated using the CO_2-H_2O equilibrium vapor saturation model (Figure 6). There are several possible reasons for this. One possibility is that the apparent undersaturation of the lavas could relate to limitations of the solubility model [*Kendrick et al.*, 2014]. Alternatively, following eruption at a shallower depth—which is assumed to be represented by the calculated CO_2-H_2O equilibrium vapor saturation pressure—the lavas could have flowed downslope so that they were dredged at greater depths than the original eruption depth (this is not unlikely, as the dredges were placed on the deep flanks of the seamounts, far below their respective summits). More likely, however, is that following eruption at shallow depth, the lithosphere thermally subsided so that the sample was dredged at greater depth than the original eruption depth; a similar model invoking seamount subsidence was suggested recently to explain shallow eruption depths (inferred from calculated CO_2-H_2O equilibrium solubility pressures) for deeply recovered glasses in Louisville seamount drill cores [*Nichols et al.*, 2014b].

4.1.2. Evaluating Evidence for Assimilation

4.1.2.1. Role of Assimilation in Modifying H_2O and Cl in Lavas

Assimilation of seawater, brines, and altered oceanic crust can modify the H_2O content of a melt, so it is important to evaluate whether the difference in H_2O/Ce ratios between the HIMU Tuvalu glasses and the HIMU Mangaia melt inclusions is a result of assimilation. Relative to pristine mantle melts, Cl is enriched in seawater, brines, and altered oceanic crust, and assimilation of these materials can increase the Cl content of a melt [*Michael and Schilling*, 1989; *Jambon et al.*, 1995; *Michael and Cornell*, 1998; *Kent et al.*, 1996a, 1992b; *Lassiter et al.*, 2002; *Stroncik and Haase*, 2004; *Kendrick et al.*, 2013]. Therefore, the abundance of Cl and the ratio of Cl to similarly incompatible elements—including K and Nb—are important for evaluating the role for assimilation in oceanic lavas. K and Nb are thought to be similarly incompatible to Cl during mantle melting, and Cl/K and Cl/Nb ratios measured in glasses should be similar to the mantle source in lavas that have experienced little or no assimilation. However, Cl/K and Cl/Nb ratios in lavas can be used to evaluate whether they have experienced assimilation.

Previous studies have demonstrated that mixing models can place powerful constraints on the magnitude and type of assimilation experienced during magma ascent and emplacement. In the current study, the high Cl/K (0.14–0.23) and Cl/Nb (21.9–32.5) of mildly HIMU lavas from Dredge 10 indicate that they probably assimilated seawater-derived Cl, but the data are inconclusive regarding the possible presence of assimilated Cl in the other lavas presented here, including the more extreme HIMU lavas (which have lower Cl/K and Cl/Nb) from dredge 10 (Figure 7). For example, the most extreme HIMU glasses from this study, from dredge 10, have Cl/K ratios (0.11–0.12) that are close to values of ∼0.1 suggested for pristine melts unaffected by assimilation [*Kamenetsky and Eggins*, 2012; *Kendrick et al.*, 2012; *Michael and Cornell*, 1998]. Cl/Nb ratios in the same glasses are also relatively low (12.8–13.7). This is an important observation, as these three glasses have the most extreme HIMU signatures reported in this study. However, if the dredge 10 HIMU glasses did assimilate a small amount of seawater-derived Cl, then the moderately high Cl/K of these lavas (Figure 7) [*Michael and Cornell*, 1998; *Kendrick et al.*, 2012], together with their low H_2O/K_2O (and low H_2O/Ce), suggests they would have assimilated brines rather than any other source of seawater-derived Cl (Figure 7). Nonetheless, the mantle-like Br/Cl of 2.4×10^{-3} and I/Cl of 5–6×10^{-5} in samples D10–36 and D10–48 (supporting information Table S3) make it unlikely that a significant component of brine was assimilated into these extreme HIMU melts. Additionally, Cl exhibits strong correlations with other highly incompatible elements (e.g., Nb) in the new data set of Tuvalu glass (not shown), and this would not be expected if seawater-derived components dominated the Cl budget (because seawater is rich in Cl but has very little Nb).

In general, Cl/K ratios correlate with Cl/Nb ratios in the new glass suite, but the dredge 5 glasses have high Cl/K ratios (0.15) at a given Cl/Nb ratio (10). If Cl is slightly more incompatible than K, then low degrees of melting might elevate the Cl/K in the melt relative to the mantle source. However, if Cl and Nb are more similarly incompatible, Cl/Nb ratios will more reliably record mantle source compositions, even at low degrees of melting [e.g., *Rowe and Lassiter*, 2009]. Thus, if low degrees of melting generated the dredge 5 melts, Cl/Nb may better record the mantle source compositions prior to assimilation than Cl/K, and the low Cl/Nb of these melts suggests that they have experienced minimal assimilation.

Previous quantification of the H_2O and Cl introduced into magmas by brine assimilation indicates that brine assimilation is expected to have a much smaller effect on H_2O/K_2O (and H_2O/Ce) than Cl/K ratios (Figure 7) [Le Voyer et al., 2014a; Kendrick et al., 2015]. Furthermore, for dredge 10 HIMU lavas, the low H_2O/Ce ratios (75–84) do not favor introduction of assimilated H_2O (from seawater or altered oceanic crust), as these low H_2O/Ce ratios are already at the low end identified in deeply dredged global OIB lavas [Workman et al., 2006; Kendrick et al., 2014, 2015]. However, the lower H_2O/Ce and H_2O/K_2O in the dredge 10 HIMU glasses compared to the Mangaia melt inclusions could potentially be explained if Mangaia melts assimilated material with high H_2O/Cl ratios, as is found in seawater and altered oceanic crust. Indeed, the Mangaia melt inclusions fall along mixing trajectories defined by assimilation of seawater and altered oceanic crust (Figure 7), and seawater and altered oceanic crust assimilation would increase H_2O/K_2O (and H_2O/Ce) in the Mangaia melt inclusions while preserving the relatively low Cl/K (0.08 ± 0.03) [Cabral et al., 2014].

Alternatively, the higher H_2O/Ce and H_2O/K_2O of Mangaia melt inclusions, compared to Tuvalu dredge 10 HIMU glasses, might relate to their primary magmatic compositions. If this is the case, then the different HIMU mantle sources sampled by Tuvalu HIMU glasses and Mangaia HIMU melt inclusions have different H_2O/Ce. We explore possible mechanisms for generating heterogeneous H_2O/K_2O and H_2O/Ce in the various HIMU mantle domains in section 4.2.

4.1.2.2. Variable F/Nd in Tuvalu HIMU Lavas

F and Nd are thought to be similarly incompatible, and the F/Nd ratio measured in a mantle melt is considered to reflect the mantle source [*Workman et al.*, 2006]. F/Nd exhibits heterogeneous compositions in the Tuvalu lavas. The elevated F/Nd ratios (36 ± 4, 2σ) in the dredge 10 glasses with the strongest HIMU signature is similar to the elevated F/Nd ratios previously reported in HIMU end-member melt inclusions from Mangaia (30 ± 9) [*Cabral et al.*, 2014]. Together, data from the Mangaia melt inclusions and Tuvalu dredge 10 lavas suggest that high F/Nd ratios may be a characteristic of HIMU lavas.

Dredge 5 lavas have slightly less extreme HIMU signatures than dredge 10 lavas and have lower F/Nd ratios (∼24). If high F/Nd relates to a stronger HIMU signature in the mantle source, then one possible hypothesis is that the lower F/Nd in the dredge 5 glasses relates to the diminished HIMU Pb-isotopic signature compared to the more extreme HIMU glasses from Dredge 10 (F/Nd = 36 ± 4) and extreme HIMU melt inclusions from Mangaia (F/Nd = 30 ± 9). However, it appears that high F/Nd ratios are not uniquely associated with extreme HIMU signatures: glasses with moderate HIMU signatures (from dredge 15) have the highest F/Nd ratios (37 ± 2) in this study. Other Tuvalu lavas with a mild HIMU signature (i.e., dredge 10 mildly HIMU glasses), or no clear HIMU signature (i.e., dredge 21 glasses), have F/Nd ratios that are low, with average values of 24 and 20, respectively. It is notable that these lavas—the dredge 10 mildly HIMU lavas and the dredge 21 lavas—have the highest Cl/K ratios (from 0.14 to 0.23) in this study (Figure 8), which may relate to enhanced assimilation, yet these lavas have among the lowest F/Nd in this study.

The origin of the F/Nd variability in the Tuvalu HIMU lavas is not clear, but it does not appear to relate to assimilation. Isolated OIBs with very high F/Nd ratios of 35–180 have been reported for melt inclusions previously [*Koleszar et al.*, 2009; *Lassiter et al.* 2002]. We note that, in contrast to Cl and H_2O, F is very unlikely to be influenced by seawater assimilation because F has a very low solubility in seawater [*Seyfried and Ding*, 1995]. As a result, seawater-derived vent fluids have very low F/Cl ratios of <0.0001 [*Edmond et al.*, 1979; *Von Damm*, 1988; *Mottl et al.*, 2011; *Reeves et al.*, 2011] and all the F present in altered oceanic crust is essentially mantle derived. Thus, the origin of the elevated F/Nd reported in this study and in previous studies [*Koleszar et al.*, 2009, *Lassiter et al.*, 2002] is still poorly understood.

However, it has previously been shown that F is subducted into the mantle preferentially relative to Cl and with moderate efficiency [*Straub and Layne*, 2003] and it is therefore possible that recycled components in the mantle might be characterized by higher than MORB F/Nd. However, F/Nd is not correlated with Pb-isotopic compositions in this study. Alternatively, if F is slightly more incompatible than Nd during mantle melting, then very low-degree melting will generate higher F/Nd ratios in the melts relative to the mantle source; if glasses in this study result from such low degrees of melting, and if F is slightly more incompatible than Nd during the melting [e.g., *Hauri et al.*, 2006; *Dalou et al.*, 2012; *Beyer et al.*, 2012; *Rosenthal et al.*, 2015], the elevated F/Nd in a subset of the glasses in this study may be a result of melting processes. Due to the fact that the extent of F/Nd variation in the mantle is still poorly defined, further work is required to evaluate these hypotheses.

4.2. Explaining the Different H_2O/Ce Ratios in Mangaia and Tuvalu HIMU Mantle Sources
4.2.1. Heterogeneous HIMU Mantle Domains With Variable H_2O/Ce
A possible explanation for the different H_2O/Ce ratios observed in Mangaia HIMU melt inclusions (higher H_2O/Ce) and the HIMU Tuvalu dredge 10 glasses (lower H_2O/Ce) is that HIMU domains in the mantle have heterogeneous H_2O/Ce. If HIMU mantle domains form by subduction of oceanic crust, variable subduction zone processes (operating in different subduction zones with different thermal regimes at different times) might generate heterogeneous subducted slab compositions. For example, H_2O loss relative to Ce may be more efficient at some subduction zones compared to others [*Hacker*, 2008]. This might be expected to generate heterogeneous trace element ratios, including H_2O/Ce, in the subducted slab that enters the convecting mantle, thereby contributing to heterogeneous HIMU reservoirs that form from these subducted slabs.

Postsubduction diffusive water loss of H_2O, but not Ce, from HIMU mantle domains may provide an additional mechanism for generating heterogeneous H_2O/Ce in different HIMU domains. Following subduction, diffusive H_2O (but not Ce) loss from the slab will commence, owing to the high diffusivity of H_2O (but not Ce) in the mantle. This mechanism will modify H_2O/Ce ratios in the subducted slab during long-term residence in the mantle [*Workman et al.*, 2006; *Shaw et al.*, 2010; *Cabral et al.*, 2014]. The process of H_2O loss by diffusion may be significant. *Cabral et al.* [2014] calculated that a 7 km-thick oceanic crustal section can lose ∼90% of its H_2O budget by diffusion to the ambient mantle over 2.5 Ga. Diffusive loss of H_2O from subducted crust can generate heterogeneous H_2O/Ce in the resulting HIMU reservoirs that evolve from the subducted oceanic crust. For example, if two different slabs with the same geometry and the same initial H_2O/Ce are stored for different lengths of time in the mantle, they will experience different degrees of water loss that will generate variable H_2O/Ce in the different HIMU reservoirs that are derived from the two slabs. Alternatively, if the geometries of the recycled subducted slabs sourcing the different HIMU domains are different, then the diffusive H_2O loss and the resulting H_2O/Ce ratios will be different in different HIMU domains even if they had the same initial H_2O/Ce and were stored for the same length of time in the mantle. For example, H_2O-loss by diffusion from the slab will be reduced for thicker slabs or for slabs piled on top of each other in the deep mantle (thus lengthening the effective diffusive distance). Thus, relative to isolated thinner slabs, slabs that have piled up on other slabs in the deep mantle will experience enhanced diffusive loss of H_2O.

In summary, differences in the subduction processes operating on subducting slabs can modify the H_2O/Ce ratio of the slab that ultimately enters the convecting mantle. Alternatively, differences in slab geometry or storage times in the mantle will result in variable H_2O loss by diffusion, which can generate different H_2O/Ce ratios in subducted slab reservoirs. If HIMU reservoirs in the mantle are comprised of subducted slabs, then it might be expected that different HIMU domains have different H_2O/Ce ratios. This conceptual model may help explain the different H_2O/Ce ratios observed in Mangaia HIMU melt inclusions and dredge 10 HIMU glasses from the Tuvalus.

4.2.2. Global Implications for H_2O/Ce Ratios in the Oceanic Mantle
The low H_2O/Ce ratios (75–84) found in the dredge 10 HIMU glasses from the Tuvalu Islands are similar to low H_2O/Ce ratios measured in the most extreme glass samples from the EM1 and EM2 mantle endmembers (approximately 50–80 in EM1 and EM2 lavas from Pitcairn, Societies, and Samoa) [*Workman et al.*, 2006; *Kendrick et al.*, 2014, 2015]. If the Mangaia inclusions have assimilated seawater (and their high H_2O/Ce does not reflect pristine HIMU melt compositions), then the new HIMU data from the Tuvalus suggest that all canonical OIB mantle end-members (EM1, EM2, and HIMU) [*Zindler and Hart*, 1986] have similar, low H_2O/Ce ratios that define the lowest H_2O/Ce in the oceanic mantle. We consider the implications of this hypothesis below.

The observation of low H_2O/Ce in EM1, EM2, and HIMU might be explained by the presence of a significant pyroxenite component in the mantle sources of the melts sampling the end-members. *Bizimis and Peslier* [2015] argued that pyroxenite cumulates have low H_2O/Ce ratios, owing to a higher bulk partition coefficient for Ce compared to H ($D_{Ce} > D_H$) during crystallization of pyroxene-rich lithologies in magma chambers in the oceanic crust, as H_2O is more incompatible than Ce in cpx [*Bizimis and Peslier*, 2015]. They suggest a pyroxenite H_2O/Ce ratio of ∼59, but in contrast, they argue that peridotites have higher H_2O/Ce ratios, based on the observation that MORB-related melts [e.g., *Michael*, 1995; *Danyushevsky et al.*, 2000; *Simons et al.*, 2002; *Ingle et al.*, 2010] that are predominantly melts of peridotite [*Salters and Stracke*, 2004; *Workman and Hart*, 2005] have higher H_2O/Ce (≥ 150). *Bizimis and Peslier* [2015] also argued that the variability of H_2O/Ce in global oceanic lavas might be explained by mixing between peridotite mantle sources (with high
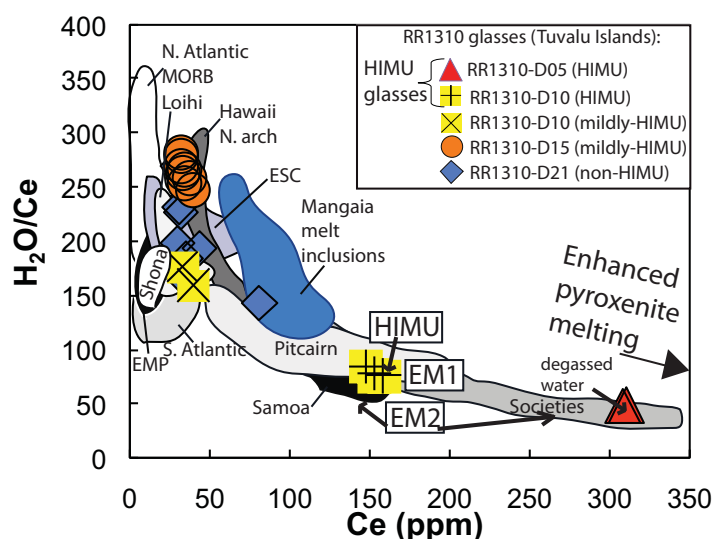
Figure 11. H$_2$O/Ce versus Ce in Tuvalu glasses and global MORB and OIB lavas. Lower H$_2$O/Ce in oceanic lavas may be associated with pyroxenite mantle source; pyroxenite melts may contribute more to erupted lavas when low degree melting operates, thus generating basalts with higher Ce and lower H$_2$O/Ce. Dredge 5 glasses may have degassed significant H$_2$O by closed-system degassing. Melt inclusion data are not shown in the figure, owing to possible open-system behavior of H$_2$O in olivine-hosted melt inclusions. However, the field for HIMU melt inclusions from Mangaia (*Cabral et al.* [2014] is shown for reference, and excludes melt inclusions that have experienced diffusive H$_2$O-loss through the host olivine (i.e., all inclusions from sample MGA-B-47). Data sources and data treatment follow Figure 9.

H$_2$O/Ce) and pyroxenite mantle sources (with low H$_2$O/Ce), consistent with previous work [*Allègre and Turcotte*, 1986; *Hauri*, 1996; *Hirschmann and Stolper*, 1996; *Salters and Dick*, 2002; *Ito and Mahoney*, 2005; *Prytulak and Elliott*, 2007; *Jackson and Dasgupta*, 2008]. If heterogeneous mixtures of peridotite and mafic materials exist in the mantle sources of all hotspots, then low degrees of melting, possibly caused by lower mantle potential temperatures and/or shorter melting columns (due to a thicker lithosphere), will preferentially sample more fusible pyroxenite components relative to the peridotite components owing to lower solidus temperatures for mafic materials [*Hirschmann and Stolper*, 1996; *Yaxley*, 2000; *Phipps Morgan*, 2001]. In addition to having lower H$_2$O/Ce, recycled mafic materials may exhibit more extreme time-integrated radiogenic isotopic compositions. Thus, lower degrees of melting may preferentially sample mantle domains that are pyroxenite rich and that have low H$_2$O/Ce and extreme radiogenic isotopic compositions, like that observed in EM1, EM2, and HIMU.

Supporting this hypothesis, a plot of H$_2$O/Ce versus Ce shows that the most extreme EM1 (Pitcairn), EM2 (Samoan and Societies), and HIMU (Tuvalu) lavas anchor the low H$_2$O/Ce and high Ce portion of a mantle array (Figure 11). In contrast, OIB and MORB melts sampling less extreme radiogenic isotopic compositions (such as lavas from Discovery, Shona, Easter Seamount Chain-Easter Microplate, North Atlantic MORB, etc.) tend to have higher H$_2$O/Ce ratios [*Bizimis and Peslier*, 2015] and lower Ce concentrations (Figure 11). We propose a conceptual model whereby the global mantle array, observed in a plot of H$_2$O/Ce versus Ce (Figure 11), may represent mixing between low degree melts (with low H$_2$O/Ce and high Ce) that preferentially sample pyroxenite lithologies and high degree melts (with high H$_2$O/Ce and low Ce) sampling a larger component of peridotite lithologies. In Figure 11, lower Ce concentrations observed in MORB and nonendmember OIB, which sample less extreme radiogenic isotopic compositions than the end-member OIB (EM1, EM2, and HIMU), are consistent with higher degrees of melting of peridotite with higher H$_2$O/Ce ratios. At the other end of the H$_2$O/Ce versus Ce array, higher Ce concentrations in EM1, EM2, and HIMU are consistent with lower degrees of melting, which concentrate incompatible elements in the melt relative to higher degree melts (particularly when melting pyroxenite lithologies, which tend to have higher Ce concentrations than peridotite lithologies). This model is supported by previous work suggesting that the mantle end-members represented by melts at Pitcairn (EM1), Societies (EM2), Samoa (EM2), and the Cook-Australs (HIMU) host a significant pyroxenite component [*Prytulak and Elliott*, 2007].

Subduction of oceanic crust is an important process for delivery of H$_2$O into the mantle. If HIMU lavas sample ancient oceanic crust that was subducted into the mantle and returned to the shallow mantle and melted beneath hotspots, then it is critical to constrain the H$_2$O/Ce ratio in HIMU lavas to place constraints on the recycling efficiency of H$_2$O into the mantle [*Dixon et al.*, 2002; *Workman et al.*, 2006; *Cabral et al.*, 2014]. With existing data, it is not possible to determine the mechanism(s) that operated to generate the different H$_2$O/Ce ratios between the Tuvalu HIMU glasses and the Mangaia HIMU melt inclusions. It is critical to evaluate whether the Mangaia melt inclusions have elevated H$_2$O/Ce as a result of assimilation processes

(section 4.1.2). If the high H_2O/Ce in Mangaia melt inclusions relative to the dredge 10 HIMU Tuvalu glasses are a result of assimilation processes having operated on the melt inclusions, then the H_2O/Ce of the dredge 10 HIMU glasses from the Tuvalus best represent the composition of the HIMU mantle. However, if high H_2O/Ce of the Mangaia melt inclusions represents a pristine melt composition unaffected by assimilation, and if the dredge 10 HIMU glasses also represent primary H_2O/Ce ratios, then the different HIMU mantle domains host variable H_2O/Ce. If heterogeneous H_2O/Ce in HIMU melts is a primary magmatic signature, then diffusion of H_2O in the HIMU mantle (section 4.2.2) and/or lithological heterogeneity (variable peridotite to pyroxenite ratios; section 4.2.2) in the HIMU mantle may be responsible for heterogeneous H_2O/Ce in HIMU melts.

5. Conclusions

Based on new geochemical measurements of a unique set of glass samples from the Tuvalu Islands, we make the following conclusions:

1. A subset of the glasses dredged in the Tuvalu Islands have the most extreme HIMU signatures identified in deeply dredged glasses to date. These HIMU glasses permit the first study of the volatile budgets of HIMU melts.
2. Primary melt CO_2 and S concentrations cannot be inferred from volatile measurements of the Tuvalu glasses. The Tuvalu glasses are all saturated in CO_2 and have experienced significant CO_2 degassing. Additionally, the Tuvalu glasses exhibit evidence for sulfide saturation, in which case the S concentrations in the glasses are buffered by sulfide.
3. F/Nd ratios in the Tuvalu glasses (from dredge 10) with the most extreme HIMU signatures are relatively high (36 ± 4). This supports the hypothesis that HIMU lavas have high F/Nd ratios. Highly heterogeneous F/Nd in the suite of Tuvalu glasses from the four dredge localities suggests that F/Nd ratios are quite variable in OIB lavas.
4. Cl/K ratios in the Tuvalu HIMU glasses (averaging 0.11 in dredge 10 HIMU glasses and 0.15 in dredge 5) are at the upper limit of Cl/K ratios in pristine OIB and MORB lavas ($\sim$0.1). Br/Cl (0.0024) and I/Cl (5–6×10^{-5}) ratios, which are sensitive to assimilation, do not support a role for assimilation in the dredge 10 lavas, which exhibit the most extreme HIMU signatures in this study. The other glasses examined in this study exhibit low Cl/K ratios, except for the mildly HIMU lavas from dredge 10, which have high Cl/K (0.14–0.23) and Cl/Nb (22–32) ratios consistent with assimilation.
5. The Tuvalu glasses with the most extreme HIMU signatures exhibit low H_2O/Ce ratios, averaging 49 (dredge 5 glasses) and 79 (dredge 10 HIMU glasses) in two different dredges. The low H_2O/Ce ratios in the dredge 5 glasses may result from H_2O-loss by degassing. However, the low ratios in the dredge 10 HIMU lavas (the lavas with the most extreme HIMU signatures in this study) are unlikely to be a result of degassing of H_2O.
6. The H_2O/Ce ratios in dredge 10 Tuvalu HIMU glasses (75–84) is lower than the ratio in olivine-hosted HIMU melt inclusions from Mangaia (119–245), even though a subset of the Mangaia HIMU melt inclusions has Pb-isotopic compositions that overlap with the most extreme glasses from the Tuvalus. The exact mechanism responsible for the lower H_2O/Ce ratio in the Tuvalu glasses relative to the Mangaia inclusions remains unknown. However, the different H_2O/Ce ratios in these separate HIMU melts may be a result of variable processes operating on the HIMU melts (i.e., the HIMU Mangaia melt inclusions may have experienced assimilation prior to entrapment, which can increase H_2O/Ce) or processes operating on the HIMU mantle sources (i.e., variable diffusive loss of H_2O, but not Ce, from different HIMU domains) to generate the observed heterogeneous H_2O/Ce.
7. If the high H_2O/Ce in the Mangaia melt inclusions is a result of assimilation, and is not a mantle source signature for Mangaia HIMU lavas, then the data set on dredge 10 HIMU glasses from the Tuvalus suggests that HIMU lavas have low H_2O/Ce that is similar to the low H_2O/Ce in EM1 and EM2 lavas globally. A relationship between H_2O/Ce ratios and Ce concentrations in global MORB and OIB pillow glasses shows a clear mantle array, whereby the mantle end-members (EM1, EM2, and HIMU) have the lowest H_2O/Ce and the highest Ce concentrations, while MORB and OIB lavas with less extreme radiogenic isotopic compositions have higher H_2O/Ce and lower Ce concentrations. This relationship is consistent with the canonical mantle end-members sampling a recycled mafic component (which is suggested to have low H_2O/Ce) while MORB and OIB lavas with less extreme radiogenic isotopic compositions are

dominated by melt extraction from peridotite (which has higher H_2O/Ce). We suggest that the global mantle array observed in a plot of H_2O/Ce versus Ce represents mixing between low degree melts sampling dominantly pyroxenitic lithologies and high degree melts sampling dominantly peridotitic lithologies.

References

Allègre, C. J., and D. L. Turcotte (1986), Implications of a two component marble-cake mantle, *Nature*, *323*, 123–127.

Alt, J. C., and D. A. H. Teagle (1999), The uptake of carbon during alteration of ocean crust, *Geochim. Cosmochim. Acta*, *63*, 1527–1535.

Asimow, P. D., and C. H. Langmuir (2003), The importance of water to oceanic mantle melting regimes, *Nature*, *421*, 815–820.

Asimow, P. D., J. E. Dixon, and C. H. Langmuir (2004), A hydrous melting and fractionation model for mid-ocean ridge basalts: Application to the Mid-Atlantic Ridge near the Azores, *Geochem. Geophys. Geosyst.*, *5*, Q01E16, doi:10.1029/2003GC000568.

Bach, W., J. C. Alt, Y. Niu, S. E. Humphris, J. Erzinger, and H. J. B. Dick (2001), The geochemical consequences of late-stage low-grade alteration of lower ocean crust at the SW Indian Ridge: Results from ODP Hole 735B (Leg 176), *Geochim. Cosmochim. Acta*, *65*, 3267–3287.

Beyer, C., S. Klemme, M. Wiedenbeck, A. Stracke, and C. Vollmer (2012), Fluorine in nominally fluorine-free mantle minerals: Experimental partitioning of F between olivine, orthopyroxene and silicate melts with implications for magmatic processes, *Earth Planet. Sci. Lett.*, *337–338*, 1–9.

Bizimis, M., and A. H. Peslier (2015), Water in Hawaiian garnet pyroxenites: Implications for water heterogeneity in the mante, *Chem. Geol.*, *397*, 61–75.

Blundy J., K. V. Cashman, A. Rust, and F. Witham (2010), A case for CO_2-rich arc magmas, *Earth Planet. Sci. Lett.*, *290*, 289–301.

Bonneville, A., R. Le Suave, L. Audin, V. Clouard, L. Dosso, P. Y. Gillot., P. Janney, and K. Maamaatuaiahutapu (2002), Arago Seamount: The missing hotspot found in the Austral Islands, *Geology*, *30*, 1023–1026.

Bonneville, A., L. Dosso, and A. Hildenbrand (2006), Temporal evolution and geochemical variability of the South Pacific superplume activity, *Earth Planet. Sci. Lett.*, *244*, 251–269.

Cabral, R. A., M. G. Jackson, E. F. Rose-Koga, K. T. Koga, M. J. Whitehouse, M. A. Antonelli, J. Farquhar, J. M. D. Day, and E. H. Hauri (2013), Anomalous sulphur isotopes in plume lavas reveal deep mantle storage of Archaean crust, *Nature*, *496*, 490–493.

Cabral, R. A., M. G. Jackson, K. T. Koga, E. F. Rose-Koga, E. H. Hauri, M. J. Whitehouse, A. A. Price, J. M. D. Day, N. Shimizu, and K. A. Kelley (2014), Volatile cycling of H_2O, CO_2, F, and Cl in the HIMU mantle: A new window provided by melt inclusions from oceanic hotspot lavas at Mangaia, Cook Islands, *Geochem. Geophys. Geosyst. 15*, 4445–4467, doi:10.1002/2014GC005473.

Cartigny, P., F. Pineau, C. Aubaud, and M. Javoy (2008), Towards a consistent mantle carbon flux estimate: Insights from volatile systematics (H_2O/Ce, δD, CO_2/Nb) in the North Atlantic mantle (14° N and 34° N), *Earth Planet. Sci. Lett.*, *265*, 672–685.

Castillo, P. (2015), The recycling of marine carbonates and sources of HIMU and FOZO ocean island basalts, *Lithos*, *216–217*, 254–263.

Chan, L.-H., J. C. Lassiter, E. H. Hauri, S. R. Hart, and J. Blusztajn (2009), Lithium isotope systematics of lavas from the Cook-Austral Islands: Constraints on the origin of HIMU mantle, *Earth Planet. Sci. Lett.*, *277*, 433–442.

Chase, C. G. (1981), Oceanic island Pb: Two-stage histories and mantle evolution, *Earth Planet. Sci. Lett.*, *52*, 277–284.

Chauvel, C., W. McDonough, G. Guille, R. Maury, and R. Duncan (1997), Contrasting old and young volcanism in Rurutu Island, Austral chain, *Chem. Geol.*, *139*, 125–143.

Chavrit, D., E. Humler, Y. Morizet, and D. Laporte (2012), Influence of magma ascent rate on carbon dioxide degassing at oceanic ridges: Message in a bubble, *Earth Planet. Sci. Lett.*, *357–358*, 376–385.

Clague, D. A., J. G. Moore, J. E. Dixon, and W. B. Friesen (1995), Petrology of submarine lavas from Kilauea's Puna Ridge, Hawaii, *J. Petrol.*, *36*, 299–349.

Colin, A., P.Burnard, and B.Marty (2013), Mechanisms of magma degassing at mid-oceanic ridges and the local volatile composition (^{4}He–^{40}Ar*–CO_2) of the mantle by laser ablation analysis of individual MORB vesicles, *Earth Planet. Sci. Lett.*, *361*, 183–194.

Collerson, K. D., Q. Williams, A. E. Ewart, and D. T. Murphy (2010), Origin of HIMU and EM-1 domains sampled by ocean island basalts, kimberlites and carbonatites: The role of CO_2-fluxed lower mantle melting in thermochemical upwellings, *Phys. Earth Planet. Int.*, *181*, 112–131.

Cohen, R. S., and R. K. O'Nions (1982), Identification of recycled continental material in the mantle from Sr, Nd and Pb isotope investigations, *Earth Planet. Sci. Lett.*, *61*, 73–84.

Dalou, C., K. T. Koga, N. Shimizu, J. Boulon, and J.-L. Devidal (2012), Experimental determination of F and Cl partitioning between lherzolite and basaltic melt, *Contrib. Mineral. Petrol.*, *163*, 591–609.

Danyushevsky, L. V., S. M. Eggins, T. J. Falloon, and D. M. Christie (2000), H_2O abundance in depleted to moderately enriched Mid-Ocean Ridge magmas; Part I: Incompatible element behaviour, implications for mantle storage and origin of regional variations, *J. Petrol.*, *41*, 1329–1364.

Dasgupta, R., and M. M. Hirschmann (2006), Melting in the Earth's deep upper mantle caused by carbon dioxide, *Nature*, *440*, 659–662.

Dasgupta, R., M. M. Hirschmann, and A. C. Withers (2004), Deep global cycling of carbon constrained by the solidus of anhydrous, carbonated eclogite under upper mantle conditions, *Earth Planet. Sci. Lett.*, *227*, 73–85, doi:10.1016/j.epsl.2004.08.004.

Dasgupta, R., M. M. Hirschmann, and N. D. Smith (2007), Partial melting experiments of peridotite+CO_2 at 3 GPa and genesis of alkalic ocean island basalts, *J. Petrol.*, *48*, 2093–2124.

Dasgupta, R., M. M. Hirschmann, W. F. McDonough, M. Spiegelman, and A. C. Withers (2009), Trace element partitioning between garnet lherzolite and carbonatite at 6.6 and 8.6 GPa with applications to the geochemistry of the mantle and of mantle-derived melts, *Chem. Geol.*, *262*, 57–77, doi:10.1016/j.chemgeo.2009.02.004.

Day, J. M. D., D. G. Pearson, C. G. Macpherson, D. Lowry, and J.-C. Carracedo (2009), Pyroxenite-rich mantle formed by recycled oceanic lithosphere: Oxygen-osmium isotope evidence from Canary Island lavas, *Geology*, *37*, 555–558, doi:10.1130/G25613A.1.

Day, J. M. D., D. G. Pearson, C. G. Macpherson, D. Lowry, and J.-C. Carracedo (2010), Evidence for distinct proportions of subducted oceanic crust and lithosphere in HIMU-type mantle beneath El Hierro and La Palma, Canary Islands, *Geochim. Cosmochim. Acta*, *74*, 6565–6589, doi:10.1016/j.gca.2010.08.021.

Devey, C. W., F. Albarede, J.-L. Cheminée, A. Michard, R. Mühe, and P. Stoffers (1990), Active submarine volcanism on the society hotspot swell (west Pacific): A geochemical study, *J. Geophys. Res.*, *95*, 5049–5066.

Devey, C. W., K. S. Lackschewitz, D. F. Mertz, B. Bourdon, J.-L.Cheminee, J. Dubois, C. Guivel, R. Hekinian, and P. Stoffers (2003), Giving birth to hotsopt volcanoes: Distribution and composition of young seamoutns from the seafloor near Tahiti and Pitcairn islands, *Geology*, *31*, 395–398.

Dixon, J. E. (1997), Degassing of alkalic basalts, *Am. Mineral.*, *82*, 368–378.

Dixon, J. E., and D. A. Clague (2001), Volatiles in basaltic glasses from Loihi Seamount, Hawaii: Evidence for a relatively dry plume component, *J. Petrol.*, *42*, 627–654.

Dixon, J. E., E. M. Stolper, and J. R. Holloway (1995), An experimental study of water and carbon dioxide solubilities in mid ocean ridge basaltic liquids.1. Calibration and solubility models, *J. Petrol.*, *36*, 1607–1631.

Dixon, J. E., L. Leist, C. Langmuir, and J.-G. Schilling (2002), Recycled dehydrated lithosphere observed in plume-influenced mid-ocean-ridge basalt, *Nature*, *420*, 385–389.

Dosso, L., B. B. Hanan, H. Bougault, J.-G. Schilling, and J.-L. Joron (1991), Sr-Nd-Pb geochemical morphology between 10˚ and 17˚ N on the Mid-Atlantic Ridge: A new MORB isotope signature, *Earth Planet. Sci. Lett.*, *106*, 29–43.

Dosso, L., H. Bougault, C. Langmuir, C. Bollinger, O. Bonnier, and J. Etoubleau (1999), The age and distribution of mantle heterogeneity along the Mid-Atlantic Ridge (31–41_N), *Earth Planet. Sci. Lett.*, *170*, 269–286.

Douglass, J., J.-G. Schilling, and R. H. Kingsley (1995), Influence of the discovery and Shona mantle plumes on the southern Mid-Atlantic Ridge: Rare earth evidence, *Geophys. Res. Lett.*, *22*, 2893–2896.

Douglass, J., J.-G. Schilling, and D. Fontignie (1999), Plume-ridge interactions of the discovery and Shona mantle plumes with the southern Mid-Atlantic Ridge (40°–55° S), *J. Geophys. Res.*, *104*, 2941–962.

Dupuy, C., H. G. Barsczus, J. Dostal, P. Vidal, and J.-M. Liotard (1989), Subducted and recycled lithosphere as the mantle source of ocean island basalts from southern Polynesia, central Pacific, *Chem. Geol.*, *77*, 1–18.

Edmond, J. M., C. Measures, R. E. McDuff, L. H. Chan, R. Collier, B. Grant, L. I. Gordon, and J. B. Corliss (1979), Ridge crest hydrothermal activity and the balances of the major and minor elements in the ocean: Galapagos data, *Earth Planet. Sci. Lett.*, *46*, 1–18.

Eggler, D. (1978), The effect of CO_2 upon partial melting of peridotite in the system Na_2O-CaO-Al_2O_3-MgO-SiO_2-CO_2 to 35 Kb, with an analysis of melting in peridotite-H_2O-CO_2 system, *Am. J. Sci.*, *278*, 305–343.

Eiler J. M., K. A. Farley, J. W. Valley, E. M. Stolper, E. H. Hauri, and H. Craig (1995), Oxygen isotope evidence against bulk recycled sediment in the mantle sources of Pitcairn island lavas, *Nature*, *377*, 138–141.

Eisele J., M. Sharma, S. J. G. Galer, J. Blichert-Toft, C. W. Devey, and A. W. Hofmann (2002), The role of sediment recycling in EM-1 inferred from Os, Pb, Hf, Nd, Sr isotope and trace element systematics of the Pitcairn hotspot, *Earth Planet. Sci. Lett.*, *196*, 197–212.

Finlayson, V. A., J. G. Konter, M. G. Jackson, A. A. P. Koppers, and K. Konrad (2014), The Rurutu Hotspot: Isotopic and trace element evidence of HIMU hotspot volcanism in the Tuvalu Islands, Abstract V33C-4883 presented at 2014 Fall Meeting, AGU, San Fransico, 14–18 Dec.

Fontignie, D., and J.-G. Schilling (1991), [87]Sr/[86]Sr and REE variations along the Easter Microplate boundaries (south Pacific): Application of multivariate statistical analyses to ridge segmentation, *Chem. Geol.*, *89*, 209–241.

Frey, F. A., D. Clague, J. J. Mahoney, and J. M. Sinton (2000), Volcanism at the edge of the Hawaiian plume: Petrogenesis of submarine alkalic lavas from the North Arch volcanic field, *J. Petrol.*, *41*, 667–691.

Gaetani, G. A., and T. L. Grove (1998), The influence of water on melting of mantle peridotite, *Contrib. Mineral. Petrol.*, *131*, 323–346.

Gale, A., M. Laubier, S. Escrig, and C. H. Langmuir (2013), Constraints on melting processes and plume-ridge interaction from comprehensive study of the FAMOUS and North Famous segments, Mid-Atlantic Ridge, *Earth Planet. Sci. Lett.*, *365*, 209–220, doi:10.1016/801j.epsl.2013.01.022.

Garapic, G., M. G. Jackson, E. H. Hauri, S. R. Hart, K. A. Farley, J. S. Blusztajn, and J. D. Woodhead (2015), A radiogenic isotopic (He-Sr-Nd-Pb-Os) study of lavas from the Pitcairn hotspot: Implications for the origin of EM-1 (enriched mantle 1), *Lithos*, *228–229*, 1–11.

Gasperini D., J. Blichert-Toft, D. Bosch, A. Del Moro, D. Macera, P. Télouk, and F. Albarède (2000), Evidence from Sardinian basalt geochemistry for recycling of plume heads into the Earth's mantle, *Nature*, *408*, 701–704.

Gast, P. W., G. R. Tilton, and C. Hedge (1964), Isotopic composition of lead and strontium from Ascension and Gough Islands, *Science*, *145*, 1181–1185.

Geldmacher J., K. Hoernle, A. Klügel, P. van den Bogaard, and I. Bindeman (2008), Geochemistry of a new enriched mantle type locality in the northern hemisphere: Implications for the origin of the EM-I source, *Earth Planet. Sci. Lett.*, *265*, 167–182.

Gerbode, C., and R. Dasgupta (2010), Carbonate-fluxed melting of MORB-like pyroxenite at 2.9 GPa and genesis of HIMU Ocean Island Basalts, *J. Petrol.*, *51*, 2067–2088, doi:10.1093/petrology/egq049.

Graham, D., S. Humphris, and W. Jenkins (1992), Helium isotope geochemistry of some volcanic rocks from Saint Helena, *Earth Planet. Sci. Lett.*, *110*, 121–131.

Gillis, K. M., and L. A. Coogan (2011), Secular variation in carbon uptake into the ocean crust, *Earth Planet. Sci. Lett.*, *302*, 385–392, doi:10.1016/j.epsl.2010.12.030.

Hacker, B. R. (2008), H_2O subduction beyond arcs, *Geochem. Geophys. Geosyst.*, *9*, Q03001, doi:10.1029/2007GC001707.

Hanan, B. B., and J.-G. Schilling (1989), Easter microplate evolution: Pb isotope evidence, *J. Geophys. Res.*, *94*, 7432–7448.

Hanyu, T., and I. Kaneoka (1997), The uniform and low [3]He/[4]He ratios of HIMU basalts as evidence for their origin as recycled materials, *Nature*, *390*, 273–276.

Hanyu, T., et al. (2011), Geochemical characteristics and origin of the HIMU reservoir: A possible mantle plume source in the lower mantle, *Geochem. Geophys. Geosyst.*, *12*, Q0AC09, doi:10.1029/2010GC003252.

Hanyu, T., et al. (2014), Isotope evolution in the HIMU reservoir beneath St. Helena: Implications for the mantle recycling of U and Th, *Geochim. Cosmochim. Acta*, *143*, 232–252.

Hart, S. R. (1988), Heterogeneous mantle domains: Signatures, genesis and mixing chronologies, *Earth Planet. Sci. Lett.*, *90*, 273–296.

Hart, S. R. (2011). The mantle zoo: New species, endangered spieces, extinct species, *Mineral. Mag.*, *3*, 983.

Hauri, E. (2002), SIMS analysis of volatiles in silicate glasses. 2: Isotopes and abundances in Hawaiian melt inclusions, *Chem. Geol.*, *183*, 115–141.

Hauri, E. H. (1996), Major-element variability in the Hawaiian mantle plume, *Nature*, *382*, 415–419.

Hauri, E. H., and S. R. Hart (1993), Re-Os isotope systematics of HIMU and EMII oceanic island basalts from the south Pacific Ocean, *Earth Planet. Sci. Lett.*, *114*, 353–371.

Hauri, E. H., N. Shimizu, J. J. Dieu, and S. R. Hart (1993), Evidence for hotspot-related carbonatite metasomatism in the oceanic upper mantle, *Nature*, *365*, 221–227.

Hauri E. H., G. A. Gaetani, and T. H. Green (2006), Partitioning of water during melting of the Earth's upper mantle at H_2O-undersaturated conditions, *Earth Planet. Sci. Lett.*, *248*, 715–734.

Hémond, C., C. Devey, and C. Chauvel (1994), Source compositions and melting processes in the Society and Austral plumes (South Pacific Ocean): Element and isotope (Sr, Nd, Pb, Th) geochemistry, *Chem. Geol.*, *115*, 7–45.

Hirschmann, M. M. (2006), Water, melting, and the deep Earth H_2O cycle, *Annu. Rev. Earth Planet. Sci.*, *34*, 629–653.

Hirschmann, M. M., and E. M. Stolper (1996), A possible role for garnet pyroxenite in the origin of the "garnet signature" in MORB, *Contrib. Mineral. Petrol.*, *124*, 185–208.

Hofmann, A. W. (1997), Mantle geochemistry: The message from oceanic volcanism, *Nature*, *385*, 219–229.

Hofmann, A. W., and W. M. White (1982), Mantle plumes from ancient oceanic crust, *Earth Planet. Sci. Lett.*, *57*, 421–436.

Honda M., and J. D. Woodhead (2005), A primordial solar-neon enriched component in the source of EM-I-type ocean island basalts from the Pitcairn Seamounts, Polynesia, *Earth Planet. Sci. Lett.*, *236*, 597–612.

Ingle, S., G. Ito, J. J. Mahoney, W. Chazey III, J. Sinton, M. Rotella, and D. M. Christie (2010), Mechanisms of geochemical and geophysical variations along the western Galápagos Spreading Center, *Geochem. Geophys. Geosyst.*, *11*, Q04003, doi:10.1029/2009GC002694.

Ito, G., and J. J. Mahoney (2005), Flow and melting of a heterogeneous mantle: 2. Implications for a chemically nonlayered mantle, *Earth Planet. Sci. Lett.*, *230*, 47–63.

Jackson, M. G., and R. Dasgupta (2008), Compositions of HIMU, EM1, and EM2 from global trends between radiogenic isotopes and major elements in ocean island basalts, *Earth Planet. Sci. Lett.*, *276*, 175–186, doi:10.1016/j.epsl.2008.09.023.

Jackson, M. G., S. R. Hart, A. A. P. Koppers, H. Staudigel, J. Konter, J. Blusztajn, M. Kurz, and J. A. Russell (2007), The return of subducted continental crust in Samoan lavas, *Nature*, *448*, 684–687.

Jackson, M. G., S. R. Hart, J. G. Konter, A. A. P. Koppers, H. Staudigel, M. D. Kurz, J. Blusztajn, and J. M. Sinton (2010), The Samoan hotspot track on a "hotspot highway": Implications for mantle plumes and a deep Samoan mantle source, *Geochem. Geophys. Geosyst.*, *11*, Q12009, doi:10.1029/2010GC003232.

Jambon, A., B. Deruelle, G. Dreibus, and F. Pineau (1995), Chlorine and bromine abundance in MORB: The contrasting behaviour of the Mid-Atlantic Ridge and East Pacific Rise and implications for chlorine geodynamic cycle, *Chem. Geol.*, *126*, 101–117.

John, T., G. D. Layne, K. M. Haase, and J. D. Barnes (2010), Chlorine isotope evidence for crustal recycling into the Earth's mantle, *Earth Planet. Sci. Lett.*, *298*, 175–182, doi:10.1016/j.epsl.2010.07.039.

Kamenetsky, V. S., and S.M. Eggins (2012), Systematics of metals, metalloids, and volatiles in MORB melts: Effects of partial melting, crystal fractionation and degassing (a case study of Macquarie Island glasses), *Chem. Geol.*, *302–303*, 76–86.

Kawabata, H., T. Hanyu, Q. Chang, J.-I. Kimura, A. R. L. Nichols, and Y. Tatsumi (2011), The Petrology and geochemistry of St. Helena alkali basalts: Evaluation of the oceanic crust-recycling model for HIMU OIB, *J. Petrol.*, *52*, 791–838, doi:10.1093/petrology/egr003.

Kelley, K. A., T. Plank, L. Farr, J. N. Ludden, and H. Staudigel (2005), Subduction cycling of U, Th and Pb, *Earth Planet. Sci. Lett.*, *234*, 369–383.

Kelley, K. A., R. Kingsley, and J.-G. Schilling (2013), Composition of plume-influenced mid-ocean ridge lavas and glasses from the Mid-Atlantic Ridge, East Pacific Rise, Galápagos Spreading Center, and Gulf of Aden, *Geochem. Geophys. Geosyst.*, *14*, 223–242, doi:10.1029/2012GC004415.

Kendrick, M. A., R. Arculus, P. Burnard, and M. Honda (2013), Quantifying brine assimilation by submarine magmas: Examples from the Galapagos Spreading Centre and Lau Basin, *Geochim. Cosmochim. Acta*, *123*, 150–165, doi:10.1016/j.gca.2013.09.012.

Kendrick, M. A., M. G. Jackson, A. Kent, E. Hauri, P. Wallace, and J. Woodhead (2014), Contrasting behaviours of CO_2, S, H_2O and halogens (F, Cl, Br and I) in the enriched-mantle melts of the Pitcairn and Society seamounts, *Chem. Geol.*, *370*, 69–81.

Kendrick, M. A., M. G. Jackson, E. H. Hauri, and D. Phillips (2015), The halogen (F, Cl, Br, I) and H_2O systematics of Samoan lavas: Assimilated-seawater, EM2 and high-^{3}He/^{4}He components, *Earth Planet. Sci. Lett.*, *410*, 197–209.

Kendrick, M. A. (2012), High precision Cl, Br and I determination in mineral standards using the noble gas method, *Chem. Geol.*, *292–293*, 116–126.

Kent, A. J. R., M. D. Norman, I. D. Hutcheon, and E. M. Stolper (1999a), Assimilation of seawater-derived components in an oceanic volcano: Evidence from matrix glasses and glass inclusions from Loihi seamount, Hawaii, *Chem. Geol.*, *156*, 299–319.

Kent, A. J. R., D. A. Clague, M. Honda, E. M. Stolper, I. D. Hutcheon, and M. D. Norman (1999b), Widespread assimilation of a seawater-derived component at Loihi Seamount, Hawaii, *Geochim. Cosmochim. Acta*, *63*, 2749–2761.

Kent, A. J. R., D. W. Peate, S. Newman, E. M. Stolper, and J. A. Pearce (2002), Chlorine in submarine glasses from the Lau Basin: Seawater contamination and constraints on the composition of slab-derived fluids, *Earth Planet. Sci. Lett.*, *202*, 361–377.

Kingsley, R. H. (2002), Mantle plume-spreading ridge interaction in the southeast Pacific: Isotope and trace element geochemistry of the Easter-Salas y Gomez Seamount chain and the Easter Microplate, Ph.D. Dissertation, Univ. of Rhode Island, Narragansett.

Kingsley, R. H., and J.-G. Schilling (1998), Plume-ridge interaction in the Easter-Salas y Gomez seamount chain-Easter Microplate system: Pb isotope evidence, *J. Geophys. Res.*, *103*, 24,159–24,177.

Kogiso, T., Y., Tatsumi, G., Shimoda, and H. G., Barsczus (1997), High μ (HIMU) ocean island basalts in southern Polynesia: New evidence for whole mantle scale recycling of subducted oceanic crust, *J. Geophys. Res.*, *102*, 8085–8103.

Koleszar, A. M., A. E. Saal, E. H. Hauri, A. N. Nagle, Y. Liang, and M. D. Kurz (2009), The volatile contents of the Galapagos plume: Evidence for H_2O and F open system behavior in melt inclusion, *Earth Planet. Sci. Lett.*, *287*, 442–452, doi:10.1016/j.epsl.2009.08.029.

Konrad, K., V. A. Finlayson, A. A. P. Koppers, J. Konter, and M. G. Jackson (2014), High resolution ^{40}Ar-^{39}Ar geochronology of the Tuvalu seamount Chain: Implications for hotspot longevity and Pacific plate motion, Abstract DI34A-03 presented at 2014 Fall Meeting, AGU, San Fransico, 14–18 Dec.

Konter, J. G., and T. W. Becker (2012), Shallow lithospheric contribution to mantle plumes revealed by integrating seismic and geochemical data, *Geochem. Geophys. Geosyst.*, *13*, Q02004, doi:10.1029/2011GC003923.

Konter, J. G., B. B. Hanan, J. Blichert-Toft, A. A.P. Koppers, T. Plank, and H. Staudigel (2008), One hundred million years of mantle geochemical history suggest the retiring of mantle plumes is premature, *Earth Planet. Sci. Lett.*, *275*, 285–295.

Koppers, A. A. P., H. Staudigel, and R. A. Duncan (2003), High-resolution ^{40}Ar/^{39}Ar dating of the oldest oceanic basement basalts in the western Pacific basin, *Geochem. Geophys. Geosyst.*, *4*(11), 8914, doi:10.1029/2003GC000574.

Koppers, A. A. P., H. Staudigel, J. Phipps Morgan, and R. A. Duncan (2007), Non-linear ^{40}Ar/^{39}Ar age systematics along the Gilbert Ridge and Tokelau seamount trail and the timing of the Hawaii-Emperor bend, *Geochem. Geophys. Geosyst.*, *8*, Q06L13, doi:10.1029/2006GC001489.

Krienitz, M.-S., C.-D. Garbe-Schönberg, R. L. Romer, A. Meixner, K. M. Haase, and N. A. Stroncik (2012), Lithium isotope variations in Ocean Island BasaltsImplications for the development of mantle heterogeneity, *J. Petrol.*, *53*, 2333–2347, doi:10.1093/petrology/egs052.

Kushiro, I. (1975), On the nature of silicate melt and its significance in magma genesis: Regularities in the shift of the liquidus boundaries involving olivine, pyroxene, and silica minerals, *Am. J. Sci.*, *275*, 411–431.

Kushiro, I., Y. Syono, and S.-I. Akimoto (1968), Melting of a peridotite nodule at high pressures and high water pressures, *J. Geophys. Res.*, *73*, 6023–6029, doi:10.1029/JB073i018p06023.

Langmuir, C., et al. (1997), Hydrothermal vents near a mantle hot spot: The Lucky Strike vent field at 37° N on the Mid-Atlantic Ridge, *Earth Planet. Sci. Lett.*, *148*, 69–91.

Lassiter, J. C., E. H. Hauri, I. K. Nikogosian, and H. G. Barsczus (2002), Chlorine–potassium variations in melt inclusions from Raivavae and Rapa, Austral Islands: Constraints on chlorine recycling in the mantle and evidence for brine-induced melting of oceanic crust, *Earth Planet. Sci. Lett.*, *202*, 525–540.

Lassiter, J. C., J. Blichert-Toft, E. H. Hauri, and H. G. Barsczus (2003), Isotope and trace element variations in lavas from Raivavae and Rapa, Cook-Austral Islands: Constraints on the nature of HIMU- and EM-mantle and the origin of mid-plate volcanism in French Polynesia, *Chem. Geol.*, *202*, 115–138, doi:10.1016/j.chemgeo.2003.08.002.

le Roux, P. J., A. P. le Roex, and J.-G. Schilling (2002), Crystallization processes beneath the southern Mid-Atlantic Ridge (40–55° S), evidence for high-pressure initiation of crystallization, *Contrib. Mineral. Petrol.*, *142*, 582–602.

Le Voyer, M., E. Cottrell, K. A. Kelley, M. Brounce, and E. H. Hauri (2014a), The effect of primary versus secondary processes on the volatile content of MORB glasses: An example from the equatorial Mid-Atlantic Ridge (5°N–3°S), *J. Geophys. Res. Solid Earth*, *120*, 125–144, doi: 10.1002/2014JB011160.

Macdonald, G. A., and T. Katsura (1964), Chemical composition of the Hawaiian lavas, *J. Petrol.*, *5*, 83–133.

Mallik, A., and R. Dasgupta (2012), Reaction between MORB-eclogite derived melts and fertile peridotite and generation of ocean island basalts, *Earth Planet. Sci. Lett.*, *329–330*, 97–108, doi:10.1016/j.epsl.2012.02.007.

Mallik, A., and R. Dasgupta (2014), Effect of variable CO_2 on eclogite-derived andesite and lherzolite reaction at 3 GPa: Implications for mantle source characteristics of alkalic ocean island basalts, *Geochem. Geophys. Geosyst.*, *15*, 1533–1557, doi:10.1002/2014GC005251.

McDonough, W. F. and C. Chauvel (1991), Sample contamination explains the Pb isotopic composition of some Rurutu island and Sasha seamount basalts, *Earth Planet. Sci. Lett.*, *105*, 397–404.

McDonough, W. F., and S. S. Sun (1995), The composition of the Earth, *Chem. Geol.*, *120*, 223–253.

Metrich, N., V. Zanon, L. Creon, A. Hildenbrand, M. Moreira, and F. O. Marques (2014), Is the "Azores Hotspot" a wetspot? Insights from the geochemistry of fluid and melt inclusions in olivine of Pico basalts, *J. Petrol.*, *55*, 377–393, doi:10.1093/petrology/egt071.

Michael, P. (1995), Regionally distinctive sources of depleted MORB: Evidence from trace elements and H_2O, *Earth Planet. Sci. Lett.*, *131*, 301–320.

Michael, P. J., and J.-G. Schilling (1989), Chlorine in mid-ocean ridge magmas: Evidence for assimilation of seawater-influenced components, *Geochim. Cosmochim. Acta*, *53*, 3131–3143.

Michael, P. J., and W. C. Cornell (1998), Influence of spreading rate and magma supply on crystallization and assimilation beneath mid-ocean ridges: Evidence from chlorine and major element chemistry of mid-ocean ridge basalts, *J. Geophys. Res.*, *103*, 18,325–18,356.

Mottl, M. J., et al. (2011), Chemistry of hot springs along the Eastern Lau Spreading Center, *Geochim. Cosmochim. Acta*, *75*, 1013–1038.

Nakamura, Y., and M. Tatsumoto (1988), Pb, Nd, and Sr isotopic evidence for a multicomponent source for rocks of Cook-Austral Islands and heterogeneities of mantle plumes, *Geochim. Cosmochim. Acta*, *52*, 2909–2924.

Nichols, A. R. L., T. Hanyu, K. Shimizu, and L. Dosso (2014a), Volatiles in submarine HIMU basalts from the Austral Islands, South Pacific, Abstract V23G–05 presented at 2014 Fall Meeting, AGU, San Francisco, 14–18 Dec.

Nichols, A. R. L., C. Beier, P. A. Brandl, D. M. Buchs, and S. H. Krumm (2014b), Geochemistry of volcanic glasses from the Louisville Seamount Trail (IODP Expedition 330): Implications for eruption environments and mantle melting, *Geochem. Geophys. Geosyst.*, *15*, 1718–1738, doi:10.1002/2013GC005086.

Nishio, Y., S. Nakai, T. Kogiso, and H. Barsczus (2005), Lithium, strontium, and neodymium isotopic compositions of oceanic island basalts in the Polynesian region: Constraints on a Polynesian HIMU origin, *Geochem. J.*, *39*, 91–103.

Niu, Y., and M. J. O'Hara (2003), Origin of ocean island basalts: A new perspective from petrology, geochemistry, and mineralphysics considerations, *J. Geophys. Res.*, *108*(B4), 2209, doi:10.1029/2002JB002048.

Palacz, Z. A., and A. D. Saunders (1986), Coupled trace element and isotope enrichment in the Cook-Austral-Samoa islands, southwest Pacific, *Earth Planet. Sci. Lett.*, *79*, 270–280.

Pan, Y., and R. Batiza (1998), Major element chemistry of volcanic glasses from the Easter Seamount Chain: Constraints on melting conditions in the plume channel, *J. Geophys. Res.*, *103*, 5287–5304.

Parai, R., S. Mukhopadhyay, and J. C. Lassiter (2009), New constraints on the HIMU mantle from neon and helium isotopic compositions of basalts from the Cook-Austral Islands, *Earth Planet. Sci. Lett.*, *277*, 253–261, doi:10.1016/j.epsl.2008.10.014.

Pilet, S., M. B. Baker, and E. M. Stolper (2008), Metasomatized lithosphere and the origin of alkaline lavas, *Science*, *320*, 916–919.

Phipps Morgan, J. (2001), Thermodynamics of pressure release melting of a veined plum pudding mantle, *Geochem. Geophys. Geosyst.*, *2*, 1001, doi:10.1029/2000GC000049.

Portnyagin, M., K. Hoernle, P. Plechov, N. Mironov, and S. Khubunaya (2007), Constraints on mantle melting and composition and nature of slab components in volcanic arcs from volatiles (H_2O, S, Cl, F) and trace elements in melt inclusions from the Kamchatka Arc, *Earth Planet. Sci. Lett.*, *255*, 53–69, doi:10.1016/j.epsl.2006.12.005.

Prytulak, J., and T. Elliott (2007), TiO_2 enrichment in ocean island basalts, *Earth Planet. Sci. Lett.*, *263*, 388–403.

Reeves, E. P., J. S. Seewald, P. Saccocia, W. Bach, P. R. Craddock, W. C. Shanks, S. P. Sylva, E. Walsh, T. Pichler, and M. Rosner (2011), Geochemistry of hydrothermal fluids from the PACMANUS, Northeast Pual and Vienna Woods hydrothermal fields, Manus Basin, Papua New Guinea, *Geochim. Cosmochim. Acta*, *75*, 1088–1123.

Rosenthal A., E. H. Hauri, and M. M. Hirschmann (2015), Experimental determination of C, F, and H partitioning between mantle minerals and carbonated basalt, CO_2/Ba and CO_2/Nb systematics of partial melting, and the CO_2 contents of basaltic source regions, *Earth Planet. Sci. Lett.*, *412*, 77–87.

Roy-Barman, M., and C. J. Allègre (1995), $^{187}Os/^{186}Os$ in oceanic island basalts: Tracing oceanic crust recycling in the mantle, *Earth Planet. Sci. Lett.*, *129*, 145–161.

Rowe, M. C., and J. C. Lassiter (2009), Chlorine enrichment in central Rio Grande Rift basaltic melt inclusions: Evidence for subduction modification of the lithospheric mantle, *Geology*, *37*, 439–442.

Saal, A. E., S. R. Hart, N. Shimizu, E. H. Hauri, and G. D. Layne (1998), Pb isotopic variability in melt inclusions from oceanic island basalts, Polynesia, *Science*, *282*, 1481–1484, doi:10.1126/science.282.5393.1481.

Saal, A. E., E. H. Hauri, C. H. Langmuir, and M. R. Perfit (2002), Vapour undersaturation in primitive mid-ocean-ridge basalt and the volatile content of Earth's upper mantle, *Nature*, *419*, 451–455.

Salters, V. J. M., and H. J. B. Dick (2002), Mineralogy of the mid-ocean-ridge basalt source from neodymium isotopic composition of abyssal peridotites, *Nature*, *418*, 68–72.

Salters, V. J. M., and A. Sachi-Kocher (2010), An ancient metasomatic source for the Walvis Ridge basalts, *Chem. Geol.*, *273*, 151–167, doi:10.1016/j.chemgeo.2010.02.010.

Salters, V. J. M., and A. Stracke (2004), Composition of the depleted mantle, *Geochem. Geophys. Geosyst.*, *5*, Q05004, doi:10.1029/2003GC000597.

Salters, V. J. M., and W. White (1998), Hf isotope constraints on mantle evolution, *Chem. Geol.*, *145*, 447–460.

Salters, V. J. M., S. Mallick, S. R. Hart, C. E. Langmuir, and A. Stracke (2011), Domains of depleted mantle: New evidence from hafnium and neodymium isotopes, *Geochem. Geophys. Geosyst.*, *12*, Q08001, doi:10.1029/2011GC003617.

Schiano, P., K. W. Burton, B. Dupre, J.-L. Birck, G. Guille, and C. J. Allègre (2001), Correlated Os-Pb-Nd-Sr isotopes in the Austral-Cook chain basalts: The nature of mantle components in plume sources, *Earth Planet. Sci. Lett.*, *186*, 527–537.

Schilling, J.-G., H. Sigurdsson, A. N. Davis, and R. N. Hey (1985), Easter microplate evolution, *Nature*, *317*, 325–331.

Seyfried, W. E., and K. Ding, K. (1995), The hydrothermal chemistry of fluoride in seawater. *Geochim. Cosmochim. Acta*, *59*, 1063–1071.

Shaw, A. M., M. D. Behn, S. E. Humphris, R. A. Sohn, and P. M. Gregg (2010), Deep pooling of low degree melts and volatile fluxes at the 85° E segment of the Gakkel Ridge: Evidence from olivine-hosted melt inclusions and glasses, *Earth Planet. Sci. Lett.*, *289*, 311–322, doi: 10.1016/j.epsl.2009.11.018.

Simons, K., J. Dixon, J.-G. Schilling, R. Kingsley, and R. Poreda (2002), Volatiles in basaltic glasses from the Easter-Salas y Gomez Seamount Chain and Easter microplate: Implications for geochemical cycling of volatile elements, *Geochem. Geophys. Geosyst.*, *3*(7), 1–29, doi: 10.1029/2001GC000173.

Staudigel, H., A. Zindler, S. Hart, and T. Leslie (1984), The isotope systematics of a juvenile intraplate volcano: Pb, Nd, and Sr isotope ratios of basalts from Loihi Seamount, Hawaii, *Earth Planet. Sci. Lett.*, *69*, 13–29.

Staudigel, H., K. H. Park, M. Pringle, J. L. Rubenstone, W. H. F. Smith, and A. Zindler (1991), The longevity of the South-Pacific isotopic and thermal anomaly, *Earth Planet. Sci. Lett.*, *102*, 24–44.

Staudigel, H., T. Plank, B. White, and H. Schmincke (1996), Geochemical fluxes during seafloor alteration of the basaltic upper oceanic crust: DSDP Sites 417 and 418: Subduction: Top to Bottom, *Geophys. Monogr.*, *96*, 19–38.

Stracke, A., M. Bizimis, and V. J. M. Salters (2003), Recycling oceanic crust: Quantitative constraints, *Geochem. Geophys. Geosyst.*, *4*(3), 8003, doi:10.1029/2001GC000223.

Stracke, A., A.W. Hofmann and S.R. Hart (2005), FOZO, HIMU, and the rest of the mantle zoo, *Geochem. Geophys. Geosyst.*, *6*, Q05007, doi: 10.1029/2004GC000824.

Straub, S. M., and G. D. Layne (2003), The systematics of chlorine, fluorine, and water in Izu arc front volcanic rocks: Implications for volatile recycling in subduction zones, *Geochim. Cosmochim. Acta*, *67*, 4179–4203.

Stroncik, N. A., and K. M. Haase (2004), Chlorine in oceanic intraplate basalts: Constraints on mantle sources and recycling processes, *Geology*, *32*, 945–948, doi:10.1130/G21027.1.

Von Damm, K. L. (1988), Systematics of and postulated controls on submarine hydrothermal solution chemistry, *J. Geophys. Res.*, *93*, 4551–4561.

Wallmann, K. (2001), The geological water cycle and the evolution of marine δ^{18}O values, *Geochim. Cosmochim. Acta*, *65*, 2469–2485.

Weaver, B. L. (1991), The origin of ocean island basalt end-member compositions: Trace element and isotopic constraints, *Earth Planet. Sci. Lett.*, *104*, 381–397.

Webster, J. D., R. J. Kinzler, and E. A. Mathez (1999), Chloride and water solubility in basalt and andesite melts and implications for magmatic degassing, *Geochim. Cosmochim. Acta*, *63*, 729–738.

Wessel, P., and L. W. Kroenke (2008), Pacific absolute plate motion since 145 Ma: An assessment of the fixed hot spot hypothesis, *J. Geophys. Res.*, *113*, B06101, doi:10.1029/2007JB005499.

White, W. M. (2010), Oceanic Island basalts and mantle plumes: The geochemical perspective, *Annu. Rev. Earth Planet. Sci.*, *38*, 133–160.

White, W. M., and A. W. Hofmann (1982), Sr and Nd isotope geochemistry of oceanic basalts and mantle evolution, *Nature*, *296*, 821–825.

Witham, F., J. Blundy, S. C. Kohn, P. Lesne, J. Dixon, S. V. Churakov, and R. Botcharnikov (2012), SolEx: A model for mixed COHSCl-volatile solubilities and exsolved gas compositions in basalt, *Comput. Geosci.*, *45*, 87–97, doi:10.1016/j.cageo.2011.09.021.

Woodhead, J. D. (1996), Extreme HIMU in an oceanic setting: The geochemistry of Mangaia Island (Polynesia), and temporal evolution of the Cook-Austral hotspot, *J. Volcanol. Geotherm. Res.*, *72*, 1–19.

Woodhead, J. D., and C. W. Devey (1993), Geochemistry of the Pitcairn seamounts. I: Source character and temporal trends, *Earth Planet. Sci. Lett.*, *116*, 81–99.

Workman, R. K., and S. R. Hart (2005), Major and trace element composition of the depleted MORB mantle (DMM), *Earth Planet. Sci. Lett.*, *231*, 53–72.

Workman, R. K., S. R. Hart, M. Jackson, M. Regelous, K. A. Farley, J. Blusztajn, M. Kurz, and H. Staudigel (2004), Recycled metasomatized lithosphere as the origin of the Enriched Mantle II (EM2) end-member: Evidence from the Samoan Volcanic Chain, *Geochem. Geophys. Geosyst.*, *5*, Q04008, doi:10.1029/2003GC000623.

Workman, R. K., E. Hauri, S. R. Hart, J. Wang, and J. Blusztajn (2006), Volatile and trace elements in basaltic glasses from Samoa: Implications for water distribution in the mantle, *Earth Planet. Sci. Lett.*, *241*, 932–951, doi:10.1016/j.epsl.2005.10.028.

Workman, R. K., J. M. Eiler, S. R. Hart, and M. G. Jackson (2008), Oxygen isotopes in Samoan lavas: Confirmation of continent recycling, *Geology*, *36*, 551–554.

Yang, H.-J., F. A. Frey, and D. A. Clague (2003), Constraints on the source components of lavas forming the Hawaiian North Arch and Honolulu Volcanics, *J. Petrol.*, *44*, 603–627.

Yaxley, G. M. (2000), Experimental study of the phase and melting relations of homogeneous basalt1peridotite mixtures and implications for the petrogenesis of flood basalts, *Contrib. Mineral. Petrol.*, *139*, 326–338.

Yurimoto, H., T. Kogiso, K. Abe, H. G. Barsczus, A. Utsunomiya, and S. Maruyama (2004), Lead isotopic compositions in olivine-hosted melt inclusions from HIMU basalts and possible link to sulfide components, *Phys. Earth Planet. Int.*, *146*, 231–242.

Zindler, A., and S. Hart (1986), Chemical geodynamics, *Annu. Rev. Earth Planet. Sci.*, *14*, 493–571.

Zindler, A., E. Jagoutz, and S. Goldstein (1982), Nd, Sr and Pb isotopic systematics in a three-component mantle: A new perspective, *Nature*, *298*, 519–523.